

Synthesis and Conformational Analysis of a Conformationally Constrained Trisaccharide, and Complexation Properties with Concanavalin A

Nathalie Navarre,^[a] Nicolas Amiot,^[a, f] Anita van Oijen,^[a] Anne Imberty,^[b] Ana Poveda,^[d] Jesus Jiménez-Barbero,^[c] Alan Cooper,^[e] Margaret A. Nutley,^[e] and Geert-Jan Boons*^[a, f]

Abstract: The trisaccharide β -D-GlcNAc(1 \rightarrow 2) α -D-Man(1 \rightarrow 3)D-Man is a fragment of a biantennary glycan that is recognized by α -D-Man-specific lectins such as concanavalin A (ConA), *Lathyrus ochrus* lectin, lentil lectin, and can adopt several conformations upon binding. To probe the importance of loss of flexibility of a saccharide during binding with ConA this trisaccharide has been synthesized in a conformationally constrained form where a methylene acetal bridge mimics a GlcNAc–O-6'...Man–O-4 intramolecular hydrogen bond. Microcalorimetry measurements revealed that the conformation-

ally constrained compound has a more favorable entropy term but this term is offset by a smaller enthalpy term. NMR spectroscopic studies have shown that the cyclic compound is indeed considerably less flexible than the linear compound and both compounds adopt mainly one conformation. SYBYL software together with energy parameters appropriate for carbohydrates was used for a systematic conformational search. The

linear compound is very flexible. A clustering method determined seven main conformational families. Six possible conformational families were identified for the cyclic compound when considering the orientations of the β GlcNAc(1 \rightarrow 2)Man and $\alpha\beta$ Man(1 \rightarrow 3)Man glycosidic bonds. The central mannose residue was docked in the binding site of ConA and the complex was refined. The results are compared with crystal structures of legume lectin–oligosaccharide complexes and with the NMR and thermodynamic data.

Keywords: calorimetry • carbohydrates • lectins • molecular modeling • oligosaccharides

Introduction

Protein–carbohydrate interactions are implicated in many essential biological processes. Examples include embryogenesis, fertilization, neuronal development, hormonal activities, and cell proliferation and organization into specific tissues.

These interactions are also important in health science, and are involved in the invasion and attachment of pathogens, inflammation, metastasis, blood group immunology, and xenotransplantation. Among protein–carbohydrate complexes those involving lectins are of considerable interest because of the high specificities of their interactions.

[a] Prof. G.-J. Boons, N. Navarre, N. Amiot, Dr. A. van Oijem
The School of Chemistry, University of Birmingham
Edgbaston, Birmingham B152TT (UK)

[b] Dr. A. Imberty^[+]
CERMAV-CNRS, BP 53
F-38041 Grenoble Cedex 9 (France)

[c] Dr. J. Jiménez-Barbero
Instituto de Química Orgánica, C.S.I.C.
Juan de la Cierva 3, E-28006 Madrid (Spain)

[d] Dr. A. Poveda
Servicio Interdepartamental de Investigación
Universidad Autónoma de Madrid, Cantoblanco
E-28049 Madrid (Spain)

[e] Prof. A. Cooper, M. A. Nutley
Department of Chemistry, University of Glasgow
Glasgow G128QQ (UK)

[f] Present address:
Complex Carbohydrate Research Center, 220 Riverbend Road
Athens, Georgia, GA 30602-4712 (USA)

[+] Associated with University Joseph Fourier, Grenoble

The molecular basis of lectin–carbohydrate interactions has been widely studied^[1] but the thermodynamics of these interactions are complex and not well understood.^[2] Consequently, the prediction of binding constants is still a difficult and unreliable process. While counterexamples exist, protein–carbohydrate association is typified by a favorable enthalpy term, which is offset by an unfavorable entropy contribution. It is widely accepted that the enthalpy term arises from a large number of hydrogen bonds and extensive van der Waals interactions. Furthermore, it has been proposed that the dynamic rearrangement of water may also contribute to the enthalpy of complexation. The entropy term has been considered to arise either from solvation effects^[3] or from the loss of conformational flexibility of the carbohydrate ligand.^[4]

The majority of oligosaccharides are flexible and in many cases a lectin binds a saccharide in a secondary rather than a global minimum conformation. For example, the β GlcNAc-

(1→2) α Man(1→3)Man trisaccharide is known to adopt different conformations when crystallized in different crystal forms of *Lathyrus ochrus* lectin.^[5] Another different conformation is observed when it is complexed with animal S-lectin.^[6] It has been shown that many of these conformations do not correspond to the global lowest energy conformation of the uncomplexed trisaccharide but to secondary minima.^[7] This trisaccharide has not been cocrystallized with ConA but has been the subject of a systematic conformational search when docked in the lectin-binding site.^[8] It has been predicted that several conformations can be complexed in the lectin-binding site.

In order to study both conformational and thermodynamic aspects of protein–carbohydrate interactions, two cyclic trisaccharides have been designed (Figure 1). The design of

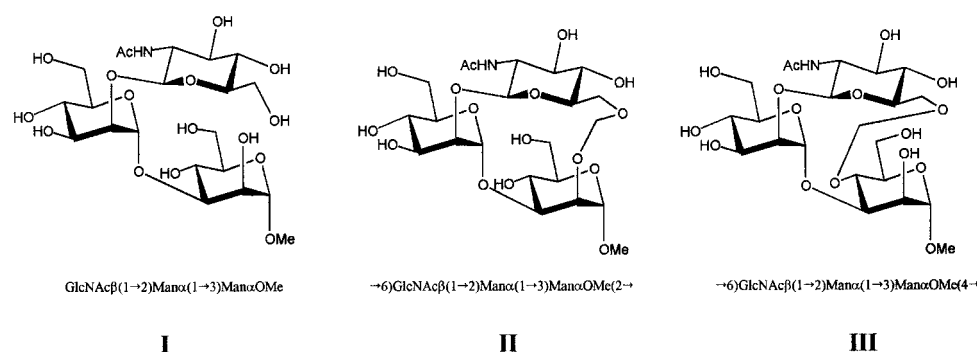


Figure 1. Schematic representation of the linear trisaccharide and the cyclic analogues.

trisaccharide **II**^[9] is based on mimicking an intramolecular hydrogen bond O2...O6'' which is present in the crystalline lectin–oligosaccharide complex^[5] by a methylene acetal. The O2...O6'' hydrogen bond is also present in a predicted docking mode of the trisaccharide to ConA.^[8] Trisaccharide **II** has been recently synthesized^[9] and its binding properties are currently under investigation.

Here, we present the synthesis of trisaccharide **III**, which contains a methylene acetal that mimics an O-4...O-6'' intramolecular bond as was predicted to occur in another possible docking mode of β GlcNAc(1→2) α Man(1→3)Man with ConA.^[8] Molecular modeling and NMR studies have demonstrated that the introduction of the methylene tether does not distort the conformation of the cyclic compound, although its flexibility is significantly reduced. On the basis of these results, it was anticipated that the conformationally constrained trisaccharide **III** would lose less conformational flexibility than the corresponding linear trisaccharide and therefore the entropic barrier associated

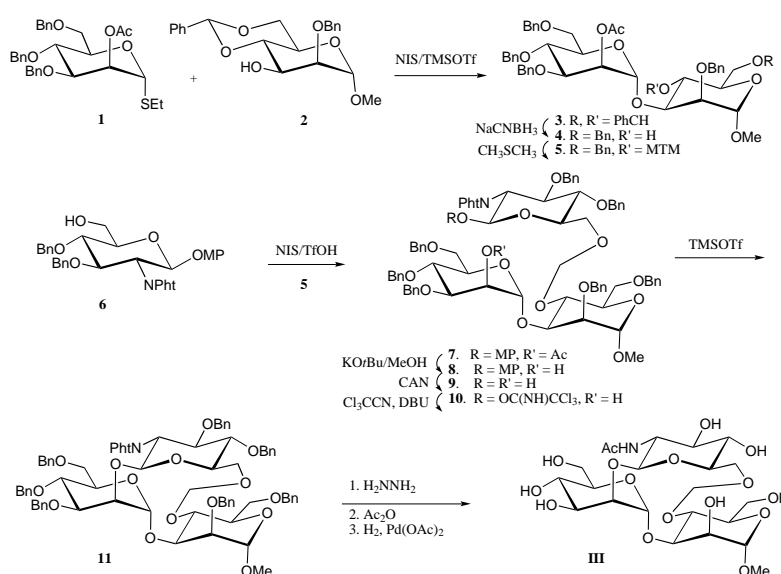
with loss of flexibility of the cyclic oligosaccharide was expected to be smaller. Indeed, the measured thermodynamic data revealed a more favorable entropy of binding of compound **III**, which surprisingly was offset by a less favorable enthalpy term.

Results and Discussion

Synthesis of the cyclic trisaccharide:

Macrocyclization is a very challenging aspect in the preparation of the conformationally restricted trisaccharide **III**. A successful approach is outlined in Scheme 1. The cyclization was achieved by an intramolecular glycosylation utilizing the precursor **10**, which already possessed a methylene acetal linker. This approach was more fruitful than macrocyclization by methylene acetal formation.

The precursor **10** for the macrocyclization was assembled from the monomeric building blocks **1**,^[10] **2**,^[11] and **6**.^[12] These compounds were readily available by standard carbohydrate protecting-group interconversion strategies. Thus, coupling of glycosyl donor **1** with glycosyl acceptor **2** in dichloromethane/ether in the presence of *N*-iodosuccinimide



Scheme 1. Synthesis of trisaccharide **III**.

(NIS)/catalytic trimethylsilyl triflate (TMSOTf)^[13] afforded the α -linked disaccharide **3** in an excellent yield (96%). The benzylidene group of **3** was selectively opened by treatment with sodium cyanoborohydride, followed by HCl in ether^[14] to give compound **4** (93%). The methylthiomethyl protecting group was introduced^[15] with dimethyl sulfide and benzoyl peroxide in acetonitrile to yield compound **5** (87%). The methylene acetal functionality was introduced by coupling of

the compounds **5** and **6** in the presence of NIS/triflic acid (TfOH), and the required saccharide **7** was obtained in a yield of 76%. Next, methylene-linked compound **7** had to be converted into a glycosyl donor suitable for an intramolecular glycosylation. To this end, the protecting group at the anomeric center of the 2-deoxy-2-phthalimidoglycosyl moiety of compound **7** had to be converted into a suitable leaving group and the 2-OH had to be deprotected. We selected an anomeric trichloroacetamido functionality as the anomeric leaving group.^[16] Thus, cleavage of the acetyl group of **7** with potassium *tert*-butoxide in methanol gave **8** and the *p*-methoxyphenyl group (MP) of **8** was removed by reaction with cerium ammonium nitrate (CAN)^[17] to afford **9**. Treatment of **9** with trichloroacetonitrile and DBU resulted in the formation of the trichloroacetimidate **10**. The regioselectivity of the latter reaction was achieved by virtue of the higher acidity of the anomeric hydroxyl group; however, care had to be taken to avoid bis(trichloroacetimidate) formation. In the following step, TMSOTf-mediated intramolecular glycosylation of **10** gave the macrocyclic compound **11** in a very good yield of 82%. Interestingly, a similar cyclization for the preparation of **II** resulted in a low yield of cyclic compound. Compound **11** was deprotected as follows: conversion of the phthalimido functionality into an NHAc moiety was accomplished by treatment with hydrazine monohydrate^[18] followed by acetylation with acetic anhydride. The benzyl ether protecting groups were removed by catalytic hydrogenation over palladium acetate to afford the requisite saccharide **III**.

The structural integrity of compound **III** was confirmed by NMR spectroscopy and FAB mass spectrometry (594, $[M+Na]^+$). The ¹H and ¹³C NMR signals were unambiguously assigned by two-dimensional homonuclear correlation spectroscopy (COSY, TOCSY). The assignments were aided by heteronuclear, proton–carbon chemical shift correlation experiments (δ (¹³C) = 103.1 ($J_{Cl, H1} = 173.5$ Hz, C-1), 102.0 ($J_{Cl', H1'} = 173.3$ Hz, C-1'), 99.6 ($J_{Cl'', H1''} = 166.4$ Hz, C-1).

Molecular modeling of the uncomplexed trisaccharides:

A four-dimensional systematic conformational search performed on the Φ and Ψ torsion angles of the β GlcNAc(1 \rightarrow 2) α Man(1 \rightarrow 3)Man trisaccharide **I** yielded 26712 conformations in a 10 kcal mol⁻¹ energy window. A cluster analysis^[8] gave seven families, and the lowest energy conformation of each of those families was fully optimized. The resulting geometries are described in Table 1. All seven conformations retained present very different geometries. The Φ and Ψ values of these conformers have been reported

Table 1. Low-energy conformations of linear trisaccharide **I** and structural characteristics (torsion angle values in ° and relative energy value in kcal mol⁻¹).

Family	Φ_{1-2}	Ψ_{1-2}	Φ_{1-3}	Ψ_{1-3}	ΔE
Linear_AA	-50.7	-171.7	68.7	99.4	0.0
Linear_AB	-51.8	-174.5	81.8	-44.6	0.8
Linear_BC	44.4	143.7	164.6	174.5	1.6
Linear_BA	44.1	146.7	68.9	104.3	2.0
Linear_BB	46.4	149.5	92.5	-39.9	2.5
Linear_BD	56.7	159.1	133.6	66.2	3.3
Linear_DC	-104.0	71.4	152.9	160.1	3.6

on the energy maps of both linkages (Figure 2) which were calculated recently^[19] with the MM3 program.^[20] For both disaccharides, the main low-energy region has been labeled A, whereas the second low-energy region has been given the label B. Regions C and D correspond to remote parts of the main low-energy region that could be considered as secondary minima. The conformations in Table 1 have been identified by the orientation of each linkage: Linear_AB corresponds to a

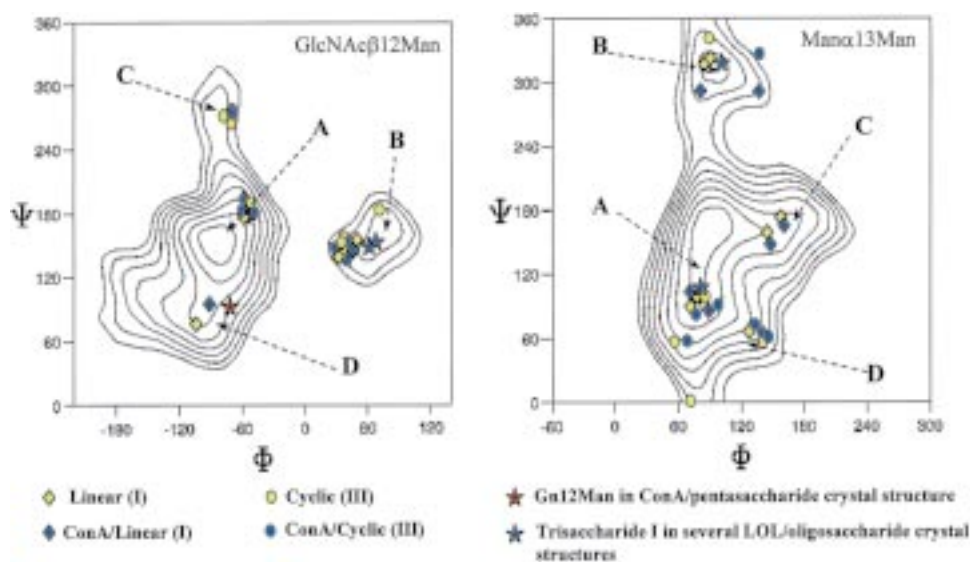


Figure 2. Superimposition of the conformations predicted for the isolated and ConA-bond trisaccharide **I** and **III** on the energy maps of each linkage, as calculated with the MM3 program.^[19] The conformations observed in some crystal structures of lectin–oligosaccharide complexes are also depicted.

conformation with the β GlcNAc(1 \rightarrow 2)Man linkage in conformation A and the α Man(1 \rightarrow 3)Man linkage in conformation B of their respective energy map.

The lowest energy conformation, Linear_AA, corresponds to the one predicted by NMR and molecular modeling studies.^[21] However, some of the other conformations are not much higher in energy. More particularly, the conformations Linear_BA and Linear_BB correspond to those observed in *N*-glycan fragments when cocrystallized with *Lathyrus ochrus* lectin.^[5, 6] The occurrence of a conformation (B on each map) that greatly differs from the absolute minimum is a characteristic of oligosaccharide flexibility. The occurrence of a small percentage of these *anti* conformers has also been demonstrated by high-resolution nuclear magnetic resonance spectroscopy (NMR). For the α -linkage, the secondary minimum corresponds to the *gauche* orientation of the Ψ angle, which has been proven to exist in solution in mannobiose^[22] and

maltose.^[23] For the β -linkages, the secondary minimum is the *gauche* conformation about the ψ angle that has been referred to as the *gauche-gauche* or alternate *exo*-anomeric effect. Independent NMR studies on the $\beta(1\rightarrow3)$ linkage,^[24] the $\beta(1\rightarrow2)$ linkage,^[25] and the *C*-analogue of the $\beta(1\rightarrow4)$ linkage^[26] in solution demonstrated the existence of the alternate conformation in addition to the usual *syn* conformer.

A systematic conformational search was run on nine of the torsion angles of the 13-membered-ring cyclic trisaccharide **III**. The Φ and Ψ torsion angles of both glycosidic linkages as well as five torsion angles of the methylene acetal bridge were rotated, resulting in 1203 conformations. After partial optimization and rejection of conformers with incorrect stereochemistry or van der Waals conflicts, 792 conformations were considered in an energy window of 10 kcal mol⁻¹. As a result of convergence during the last step of geometry optimization, only 23 conformations presented different geometries in terms of the 13-membered-ring shape and were stored. Since the acetal bridge appears to be the most flexible part of this macrocycle, the 23 conformations can be classified in six families, based on the conformation of the two glycosidic linkages (Table 2).

The conformations, grouped in six families, are displayed in Figure 3. Despite the cyclization constraints, both linkages can adopt several very different conformations in an energy window of 10 kcal mol⁻¹. For each family, the methylene acetal bridge moves freely. In order to evaluate the influence of cyclization on the conformational behavior of the glycosidic linkages, the six conformations have been reported on the energy maps of both linkages (Figure 2). From this comparison it can be seen that the cyclization does not force the linkages into high-energy regions: all the calculated conformations are encountered by the most external iso-

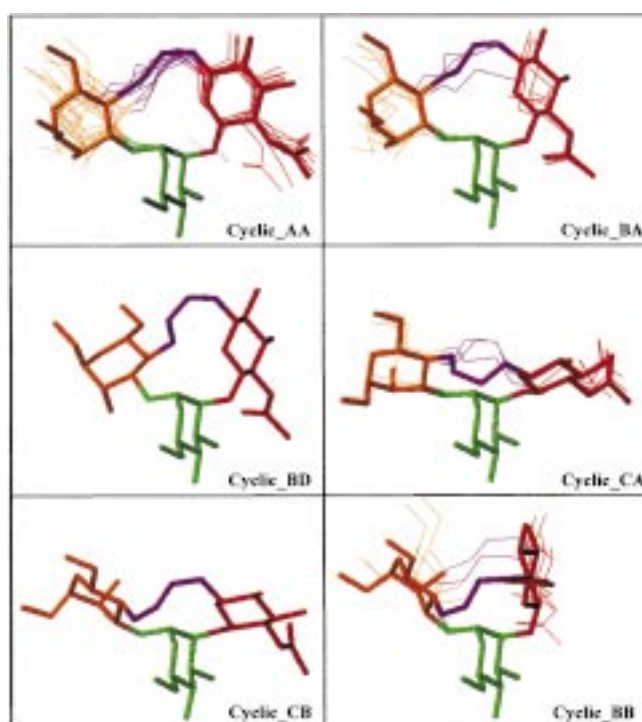


Figure 3. Graphical representation of the 23 low-energy conformers of compound **III** distributed in six families, based on the conformations of the glycosidic linkages. The lowest energy conformation of each family is represented by sticks. Color-coding is as follows: red for the β GlcNAc, green for the central α Man, and yellow for the α ManOMe; the tether is colored violet.

energy contour (8 kcal mol⁻¹). The trisaccharide is still rather flexible since many areas of the energy maps are spanned by the calculated conformations. However, there is a significant reduction of flexibility when compared with the linear trisaccharide, and, for example, the AB conformation cannot be adopted by the constrained compound.

When comparing the conformational behavior of the linear and cyclic trisaccharides, the global minimum conformation of each oligosaccharide appears to be almost identical. However, the secondary minima do not appear in the same order.

Conformational analysis by NMR spectroscopy:

The ¹H NMR and ¹³C NMR spectra were completely assigned by a combination of homonuclear COSY, TOCSY, and heteronuclear HMQC, HMBC, and HMQC-TOCSY techniques. The latter two techniques were crucial to resolve the final ambiguities. The corresponding ¹H and ¹³C NMR chemical shifts of compounds **I** and **III** are listed in Table 3.

Table 2. Low-energy conformations of cyclic trisaccharide **III**, and their classification in conformational families based on the conformation at the two glycosidic linkages (torsion angle values in ° and relative energy value in kcal mol⁻¹).

Family	Φ_{1-2}	Ψ_{1-2}	Φ_{1-3}	Ψ_{1-3}	ω_1	ω_2	ω_3	ω_4	ω_5	ΔE
Cyclic_AA	-44.4	-169.4	75.9	89.3	76.1	-74.5	128.6	159.6	-118.7	0.0
	-43.3	-168.8	62.9	84.5	56.9	80.7	-117.8	-85.9	-95.8	1.3
	-49.4	-163.7	77.8	117.5	42.3	69.1	-161.9	166.3	57.7	2.6
	-38.4	-170.7	77.5	146.1	61.0	-94.5	-162.6	-72.4	122.5	3.9
	-37.6	175.7	67.6	138.2	73.2	-44.1	-176.6	179.9	154.9	4.0
	-29.1	-172.1	97.1	86.3	-42.2	76.2	24.2	155.0	-103.8	4.2
	-47.7	-163.3	123.2	101.8	47.3	-97.5	142.5	51.8	40.2	4.8
	-38.7	-166.1	122.8	81.7	-42.6	112.2	-50.3	175.5	-37.1	8.2
	-38.6	-156.6	143.4	60.6	-44.5	107.2	-88.5	173.7	40.1	8.4
Cyclic_BA	43.0	150.4	74.0	95.3	-71.7	70.6	57.8	156.0	-129.0	0.3
	47.5	150.2	79.2	113.4	-59.7	107.0	-145.7	177.7	56.5	2.2
	66.3	-172.3	57.6	75.7	-77.2	85.8	-126.3	-168.5	64.4	3.4
	45.8	142.1	70.1	134.9	-60.6	68.2	151.1	-176.9	134.3	3.6
Cyclic_BD	45.7	147.8	68.0	93.9	-60.1	144.0	-78.6	-125.2	-89.5	3.8
	52.0	148.1	140.5	55.0	-65.6	73.4	-95.4	-144.7	66.0	2.7
Cyclic_CA	-59.6	-86.5	54.2	53.1	69.7	-131.5	57.6	142.5	52.7	3.3
	-57.0	-83.0	52.8	46.4	-56.7	76.6	40.9	165.7	-102.7	4.4
	-51.6	-77.2	51.9	63.7	-45.3	120.3	-132.8	166.7	57.7	6.4
	-54.7	-84.5	52.0	48.0	-45.4	139.5	-58.2	-134.7	-80.0	7.3
Cyclic_CB	-68.0	-96.2	74.0	1.5	49.3	75.4	-452.8	-23.9	-98.1	5.6
	Cyclic_BB	69.0	-167.0	87.4	-16.3	-63.7	112.9	-148.7	-2.3	-99.2
68.6		179.2	124.5	-30.8	-66.0	101.5	-160.9	38.9	-118.9	6.2
65.1		161.1	141.5	-26.7	-58.5	101.1	-153.7	32.4	-107.8	6.4

Table 3. 500 MHz ^1H and ^{13}C NMR chemical shifts for trisaccharides **I** and **III** at 303 K.

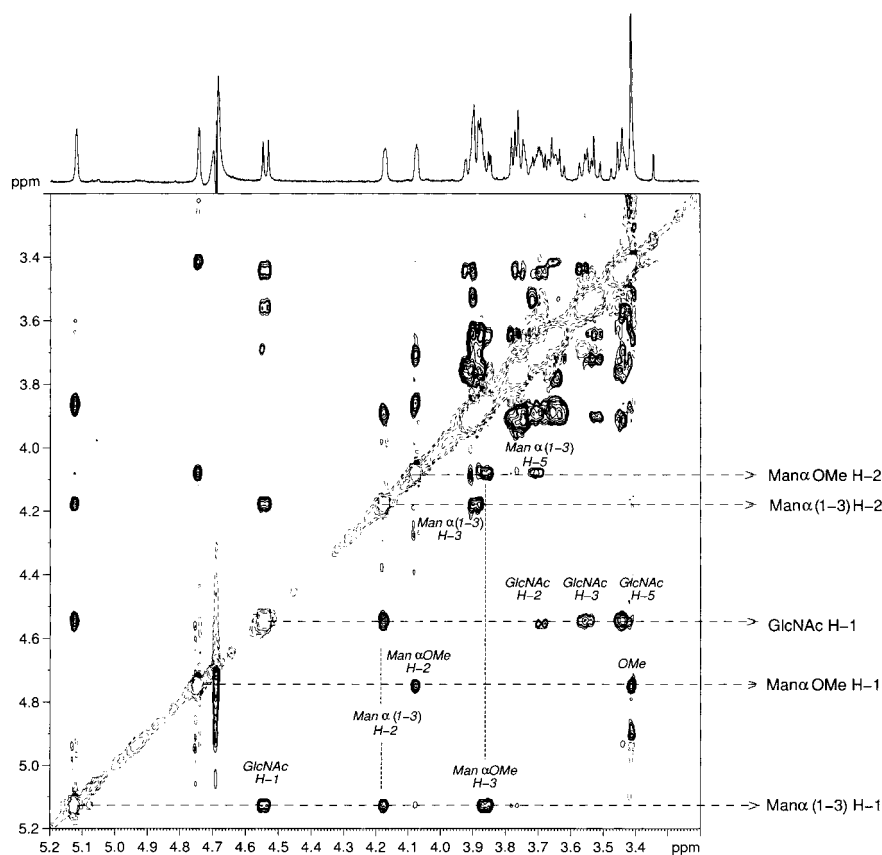
Proton	Trisaccharide I	Trisaccharide III
GlcNAc H-1	4.52/101.7	4.92/99.6
GlcNAc H-2	3.68/57.8	3.95/56.6
GlcNAc H-3	3.53/75.8	3.61/76.4
GlcNAc H-4	3.49/72.2	3.53/71.6
GlcNAc H-5	3.47/78.3	3.71/78.7
GlcNAc H-6A	3.92/63.0	4.10/70.4
GlcNAc H-6B	3.79/63.0	4.02/70.4
Man α (1 \rightarrow 3) H-1	5.12/100.3	5.68/102.0
Man α (1 \rightarrow 3) H-2	4.16/78.7	4.38/75.0
Man α (1 \rightarrow 3) H-3	3.89/71.9	4.01/71.8
Man α (1 \rightarrow 3) H-4	3.52/69.6	3.71/69.3
Man α (1 \rightarrow 3) H-5	3.69/76.0	3.72/75.7
Man α (1 \rightarrow 3) H-6A	3.91/63.6	3.97/63.4
Man α (1 \rightarrow 3) H-6B	3.64/63.6	3.86/63.4
Man α OMe H-1	4.72/102.2	4.82/103.1
Man α OMe H-2	4.06/72.0	4.10/72.5
Man α OMe H-3	3.85/80.5	4.11/77.7
Man α OMe H-4	3.75/68.2	3.84/76.9
Man α OMe H-5	3.65/75.0	3.77/74.4
Man α OMe H-6A	3.95/63.0	3.95/62.7
Man α OMe H-6B	3.78/63.0	3.84/62.7
<i>pro-R</i> CH ₂	–	5.17/100.4
<i>pro-S</i> CH ₂	–	5.03/100.4

The existence of molecular motion around the glycosidic linkages of oligosaccharides has now been firmly established.^[27–29] In addition, recent investigations have revealed that the rates of overall and internal motions of small and medium-size oligosaccharides may occur on similar time scales.^[30] Since NMR parameters are essentially time-averaged, the information that can be deduced from NOE experiments corresponds to a time-averaged conformation in solution.

For both trisaccharides, the pyranoid rings can be described as essentially monokonformational $^4\text{C}_1$, as deduced from the proton–proton coupling patterns and intrasidue NOE data. Small couplings are observed for both Man anomeric protons (< 2 Hz) and H-2 Man α (1 \rightarrow 3) (< 4 Hz), while an 8.4 Hz coupling is measured for the GlcNAc analogue. In fact, for the GlcNAc residue all proton chemical shifts (H-1 \rightarrow H-6_(S,R)) can be obtained through a TOCSY experiment as expected for an all-axial conformation of the ring protons. In addition, medium-strong H-1–H-3 and H-1–H-5 cross-peaks support the usual chair conformation. For both Man residues, the TOCSY transfer from H-1 stops at H-2

(two small consecutive $J_{\text{H}1,\text{H}2}$ and $J_{\text{H}2,\text{H}3}$), although all cross-peaks H-2 \rightarrow H-6_(S,R) can be deduced from H-2 Man α (1 \rightarrow 3), and H-2 \rightarrow H-5 connectivities from H-2 Man α OMe, as expected for the Man residues adopting the $^4\text{C}_1$ conformation. In addition, medium-strong H-1–H-2 cross-peaks are observed for both Man anomeric protons. The NOESY and ROESY experiments were used to estimate proton–proton interresidue distances qualitatively.^[31] NOESY cross-peaks are positive at 299 K and 500 MHz. (Figures 4 and 5) ^1H NMR cross-relaxation rates^[31, 32] (σ_{ROESY} and σ_{NOESY}) were obtained from the 2D-NOESY and 2D-ROESY experiments. $\sigma_{\text{ROESY}}/\sigma_{\text{NOESY}}$ ratios^[33] are independent of interproton distances and allow us to estimate specific correlation times and therefore interproton distances (see Experimental Section). For both compounds, overall correlation times around 0.2–0.3 ns were obtained. This fact indicates that both molecules tumble almost isotropically in solution and that the isolated-spin-pair approximation (ISPA) can be safely applied to deduce proton–proton distances. In fact, the results for the distances given in Tables 4–6 are very similar to those estimated by the ISPA method. The corresponding H-1–H-2 intrasidue signals were used as reference (2.4 Å) for the α -linkages, and the H-1–H-3 and H-1–H-5 intensities for the unique β -linkage. The distances calculated by molecular mechanics are also shown in Tables 4–6.

For the acyclic trisaccharide **I**, the experimentally deduced NMR distances arise from different conformational isomers (Table 4). Indeed, the observed NOEs for the Man α (1 \rightarrow 3)Man linkage (weak NOE for Man α (1 \rightarrow 3) H-1–

Figure 4. NOE spectrum of compound **I**.

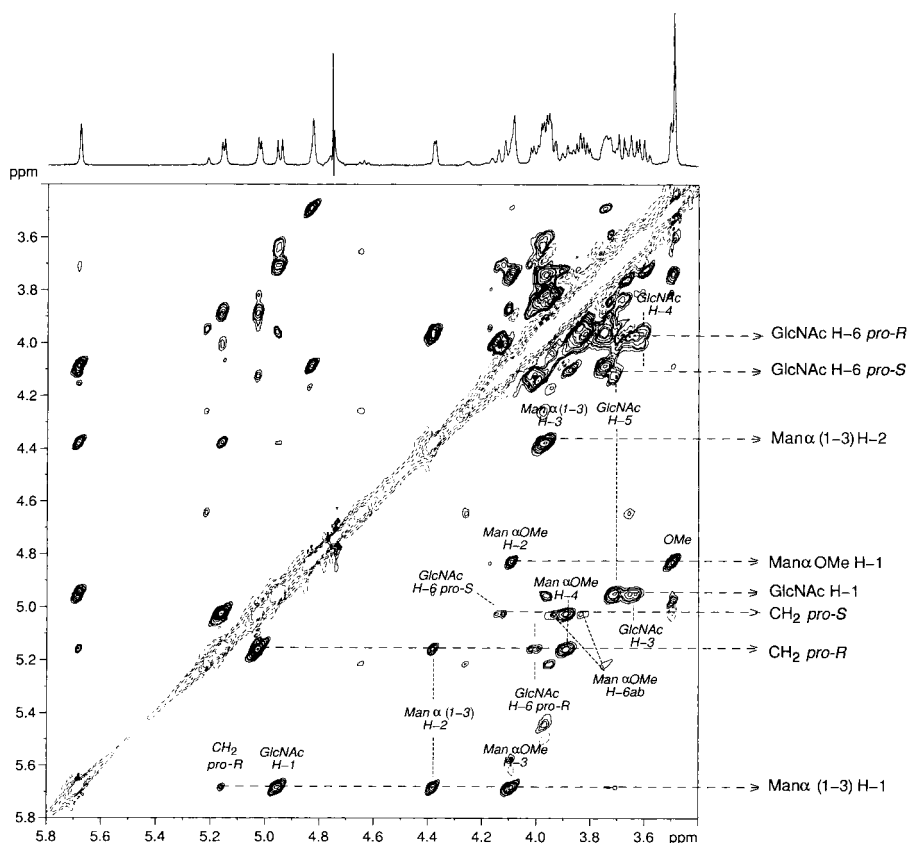
Figure 5. NOE spectrum of compound **III**.

Table 4. Experimental and calculated proton–proton distances for trisaccharide **I**. The experimental distances have been calculated from the NOE and ROE cross-relaxation rates as described in the experimental part. The calculated distances correspond to the representative structure for every local minimum. Estimated errors in the experimental distances are smaller than 5%.

H–H Pair	GlcNAc β (1 \rightarrow 2)Man α linkage				Man α (1 \rightarrow 3)Man α OMe linkage				
	Conformer				Conformer				
Exp	A	B	C	D	Exp	A	B	C	D
1–1	2.4	2.1	3.6	4.1	nd ^[a]	6.0	4.7	4.5	5.9
1–2	2.6	3.3	3.6	2.3	3.3	4.3	3.5	2.1	4.2
1–3	nd	4.8	5.3	3.8	2.2	2.4	3.6	2.9	2.4
1–4	nd	3.9	4.2	3.8	3.5	3.7	2.3	4.3	3.5
2–1	ov ^[b]	4.7	4.2	4.3	nd	7.1	6.0	5.3	6.2
2–2	nd	4.1	2.2	4.2	nd	5.2	3.9	3.3	5.0
5–2	nd	4.2	4.6	4.5	2.7	2.4	5.1	5.0	3.9

[a] nd = not determined. [b] ov = overlapping signal.

Man α OMe H-2, strong NOE for Man α (1 \rightarrow 3) H-1–Man α OMe H-3, and medium NOE for Man α (1 \rightarrow 3) H-5–Man α OMe H-2) are basically identical to those observed for the disaccharide indicating that the GlcNAc residue does not have a significant effect on the conformational behavior of this linkage. The conformation around this glycosidic linkage may be described as a conformational equilibrium around conformer A, with minor excursions towards the regions defined by conformers C and D, and in all cases the values of the Φ and Ψ angles are positive. The NOE data obtained for the GlcNAc β (1 \rightarrow 2)Man linkage unequivocally indicate that the conformation of this linkage can be described by a conformational equilibrium between conformers A and D, since both GlcNAc β H-1–Man α H-1 and GlcNAc β H-1–

Man α H-2 NOE contacts are fairly strong. Since no GlcNAc β H-2–Man α H-2 NOE is observed, conformer B is less than 5% present in solution at this linkage, within experimental error. In addition, no conformer can simultaneously satisfy the corresponding two close distances, and therefore the presence of conformational averaging between conformers A and D is firmly confirmed.

The observed NOEs for cyclic compound **III** (Tables 5 and 6) are fairly distinct for the GlcNAc β (1 \rightarrow 2)Man linkage and now the interresidue GlcNAc β H-1–Man α H-2 distance is appreciably larger than the corresponding GlcNAc β H-1–Man α H-1, as can be deduced from the relative intensities of the NOEs. Again, no GlcNAc β H-2–Man α H-2 is observed; this indicates that conformer B does not participate in the conformational

Table 5. Experimental and calculated proton–proton distances for trisaccharide **III**.

H–H Pair	GlcNAc β (1 \rightarrow 2)Man α linkage			Man α (1 \rightarrow 3)Man α linkage				
	Conformer			Conformer				
Exp	AA	BA	CA, CB	Exp	AA	BB	BD	
1–1	2.2	2.1	3.6	3.3	nd ^[a]	6.0	4.7	5.9
1–2	3.2	3.3	3.6	3.6	ov ^[b]	4.3	3.5	4.2
1–3	nd	4.8	5.3	3.6	2.2	2.4	3.6	2.4
1–4	nd	3.9	4.2	2.0	3.3	3.7	2.3	3.5
2–1	nd	4.7	4.2	4.6	nd	7.1	6.0	6.2
2–2	nd	4.1	2.2	4.5	nd	5.2	3.9	5.0
5–2	nd	4.2	4.6	5.4	ov	2.4	5.1	3.9

[a] nd = not determined. [b] ov = overlapping signal.

Table 6. Experimental and calculated proton–proton distances for the bridge methylene protons of trisaccharide **III**.

Pair	Exp	AA	BA	BB	BD	CA	CB
<i>pro-R</i> CH ₂ –Man α (1 \rightarrow 3) H-1	2.8	2.6	2.6	4.2	3.4	4.2	4.2
<i>pro-R</i> CH ₂ –Man α (1 \rightarrow 3) H-2	2.6	2.5	2.3	6.6	4.5	6.6	6.6
<i>pro-R</i> CH ₂ –GlcNAc β H-6S	3.2	3.6	3.1	3.4	4.0	3.1	2.7
<i>pro-R</i> CH ₂ –GlcNAc β H-6R	2.9	2.5	3.8	2.8	3.3	2.7	3.7
<i>pro-R</i> CH ₂ –Man α OMe H-4	2.7	2.7	2.8	3.9	3.6	3.8	3.2
<i>pro-S</i> CH ₂ –GlcNAc β H-6S	2.7	3.8	3.7	3.4	3.5	3.9	2.6
<i>pro-S</i> CH ₂ –GlcNAc β H-6R	2.9	3.1	4.1	2.2	2.2	3.6	3.6
<i>pro-S</i> CH ₂ –Man α OMe H-6AB	3.3	2.6	3.0	3.8	4.1	3.4	3.7
<i>pro-S</i> CH ₂ –Man α OMe H-4	2.8	2.3	2.1	3.3	3.9	3.6	3.5

equilibrium. According to these results, the cyclization rigidifies the GlcNAc β (1 \rightarrow 2)Man linkage and conformer A is basically the only one in solution. On the other hand, the NOEs for the Man α (1 \rightarrow 3)Man linkage are identical to the linear compound. Although there is overlapping between

Man α OMe H-3 and H-2 protons, the NOE cross-peak intensity between these resonances and Man α (1 \rightarrow 3)Man H-1 can be ascribed exclusively to the Man α OMe H-3–Man α (1 \rightarrow 3)Man H-1 cross-peak. In fact, according to the modeling results, and despite the extensive search performed (see below), no conformer with a Man α OMe H-2–Man α (1 \rightarrow 3)Man H-1 distance below 3.82 Å could be detected. This is due to the fact that conformation C around this glycosidic linkage cannot be attained because of the cyclization. Therefore, the presence of the cycle poses a major constraint around the GlcNAc β (1 \rightarrow 2)Man α linkage and now the experimental NOEs of this compound can be described by conformer AA. In the absence of J coupling data, the assignment of diastereotopic protons heavily relies on the presence of a major conformation.^[31] Thus, by considering the geometries (not the relative energies) deduced from the modeling studies, the diastereotopic methylene bridge protons could also be assigned. As mentioned above, cyclization of the trisaccharide highly restricts the GlcNAc β (1 \rightarrow 2)Man α linkage. Several NOEs were observed for the methylene bridge protons. Particularly important were those between the low-field proton with both Man α (1 \rightarrow 3) H-1 and H-2. Again, and according to the modeling results, for all the found conformers, only the *pro-R* proton may show short distances with these two protons at the Man residue, thus providing the key for diastereotopic assignment. Additional NOEs are also observed between both methylene bridge protons with Man α OMe H-4, both GlcNAc and Man α OMe H-6s, and Man α OMe H-5. The pattern of the observed NOEs between both methylene bridge protons and the GlcNAc H-6s (strong *pro-R*-high field, weak *pro-R*-low field, strong *pro-S*-low field, weak *pro-S*-high field) seems to indicate that the low-field GlcNAc H-6 proton is indeed the *pro-S* proton. This assignment is also supported by observed intraresidue NOEs between the methylene GlcNAc H-6s with H-4 and H-5, that is medium/strong high field GlcNAc H-6–H-4, medium/strong low-field GlcNAc H-6–H-5, medium/weak high field GlcNAc H-6–H-5, weak low-field GlcNAc H-6–H-4. This is the expected NOE pattern for the usual *gg/gt* equilibrium around the GlcNAc C-5–C-6 bond.^[34] The $J_{H5, H6S}$ and $J_{H5, H6R}$ of this residue are 2.0 and 4.9 Hz and therefore the experimental equilibrium is approximately *gg:gt* 60:40.^[34]

The simultaneous existence of all the aforementioned NOEs can only be explained by the presence of mobility in this region of the molecule. Therefore, a major conformer AA may explain the conformational behavior of this trisaccharide, with local flexibility around the C-6-O-CH₂-O region of the macrocycle. Although only qualitative, the geometry of this conformer may explain the unusual chemical shift observed for H-1 and H-2 of the Man α (1 \rightarrow 3) residue. These two atoms are in close proximity to O-4 Man α OMe (2.3 Å) and O-5 GlcNAc (2.5 Å). In addition, the relative deshielding of the *pro-R* methylene bridge proton with respect to the *pro-S* analogue could also be explained by its proximity to O-5 GlcNAc (2.4 Å) in the AA conformation.

The modeling results of the uncomplexed molecules are in good agreement with the experimental results, because the calculations (see above) predict an equilibrium in which conformer A is the major one for the GlcNAc β (1 \rightarrow 2)Man

linkage, while an equilibrium between conformers A and D was predicted. The calculations for compound **III** predict a major conformer AA with variation around the angles defining the methylene orientation. These predictions are consistent with the experimental data, and the only discrepancy is the absence of conformer BA, which according to the calculations should be present to some extent.

Molecular modeling of the complexes between ConA and the trisaccharides:

All conformational families determined for the linear compound **I** were docked in the ConA binding site. All of the seven tested conformations could be accommodated in the binding site with no major changes in their geometries (Table 7), except for the Linear_BD conformation, which

Table 7. Low-energy conformations of linear trisaccharide **I** and cyclic trisaccharide **III** when docked in the binding site of ConA. Hb indicates the number of hydrogen bonds between the ligand and the protein. ΔE_{tot} (kcal mol⁻¹) is the difference between the energy of the complex and the energy of the noninteracting protein and trisaccharide, whereas ΔE_{int} is the interaction energy between protein and ligand.

Conformation	Φ_{1-2}	Ψ_{1-2}	Φ_{1-3}	Ψ_{1-3}	Hb	ΔE_{tot}	ΔE_{int}
ConA–Linear_BA	52.2	151.7	71.0	102.3	8	–37.9	–45.9
ConA–Linear_BC	51.5	150.5	161.7	166.1	11	–35.4	–43.7
ConA–Linear_BB	54.3	146.5	139.3	–69.8	8	–35.0	–43.2
ConA–Linear_AA	–55.8	–166.6	89.9	87.2	6	–31.5	–38.2
ConA–Linear_AB	–52.6	–158.2	83.9	–68.6	6	–31.1	–39.2
ConA–Linear_DC	–82.8	99.5	152.6	145.7	11	–26.4	–42.3
ConA–Cyclic_BA	48.8	148.9	70.7	88.9	9	–39.2	–45.6
ConA–Cyclic_BD	52.9	149.1	141.3	55.7	10	–36.3	–42.3
ConA–Cyclic_AA	–55.9	–154.7	100.5	90.1	7	–33.4	–41.2
ConA–Cyclic_BB	57.3	147.1	156.6	–20.2	10	–31.0	–40.9
ConA–Cyclic_CA	–62.1	–83.1	60.3	61.3	11	–27.5	–47.6
ConA–Cyclic_CD	–42.6	–156.8	128.4	71.6	8	–24.2	–38.3

gave a much higher energy complex than the others. The complex with the lowest energy is ConA–Linear_BA. The preference of conformation B (the one that does not correspond to the *exo*-anomeric effect) for the β GlcNAc(1 \rightarrow 2)Man linkage is marked, since this orientation is predicted to occur in the three lowest energy docking modes. This result is in agreement with previous calculations performed on the same complex by a different approach.^[8]

The conformation of this linkage also affects the orientation of the central mannose in the binding site. When conformation B is adopted, the mannose is very deep in the binding site and all the hydrogen bonds have the characteristics observed in the ConA– α Man complex.^[35] When conformation A is taken, the mannose is not so deeply docked, probably because of steric interactions of the GlcNAc with the protein surface, and some hydrogen bonds are weaker. The GlcNAc residue also establishes hydrogen bonds with the peptide, but only if linkage β (1 \rightarrow 2) is not in conformation A. The third predicted conformation for the β GlcNAc(1 \rightarrow 2)Man is termed D. In this intermediate case, the mannose is not very deep in the binding site, but many hydrogen bonds still exist, and furthermore, the GlcNAc presents some additional hydrogen bonds with the Thr²²⁶ side chain and Gly²²⁴ backbone. It has to be noted that this peculiar conformation is the one observed for the

β GlcNAc(1 \rightarrow 2)Man disaccharide in the crystal structure of ConA–pentasaccharide complex.^[36]

All of the 23 low-energy conformations of the cyclic trisaccharide **III** were considered for the docking study with ConA. After the central mannose residue was fitted in the binding site and the energy of the complexes was optimized with appropriate energy parameters,^[37] 20 different conformers were stored in an energy window of 15 kcal mol⁻¹. The other conformers were rejected either because of their high energy or because their geometry converged close to one already considered. The conformers have been clustered in six families based on the conformation at the β GlcNAc(1 \rightarrow 2)Man and α Man(1 \rightarrow 3)Man linkages (Table 7). All conformations are displayed in Figure 6. When docked in the ConA binding site, the trisaccharide can in principle still adopt several different conformations. However, as for the linear saccharide, the B conformation of the β GlcNAc(1 \rightarrow 2)Man linkage is energetically favored in the ConA complex state.

Complexation studies of the saccharides with ConA:

Thermodynamic data obtained by isothermal microcalorimetry for complexation of the disaccharide α Man(1 \rightarrow 3) α ManOMe, the trisaccharide **I** and **III** with ConA are listed in Table 8 together with literature data for related compounds. Although the entropy and enthalpy contributions of particular interactions vary between reporting authors, some clear tendencies can be identified. First, there is a limited variation of free energy of binding between mono-, di-, and trisaccharides, a phenomenon that is attributed to entropy/enthalpy compensation. Second, binding of α Man(1 \rightarrow 3)Man-containing fragments has a more favorable enthalpy but a less favorable entropy contribution than its β GlcNAc(1 \rightarrow 2)Man counterpart. The linear trisaccharide **I**

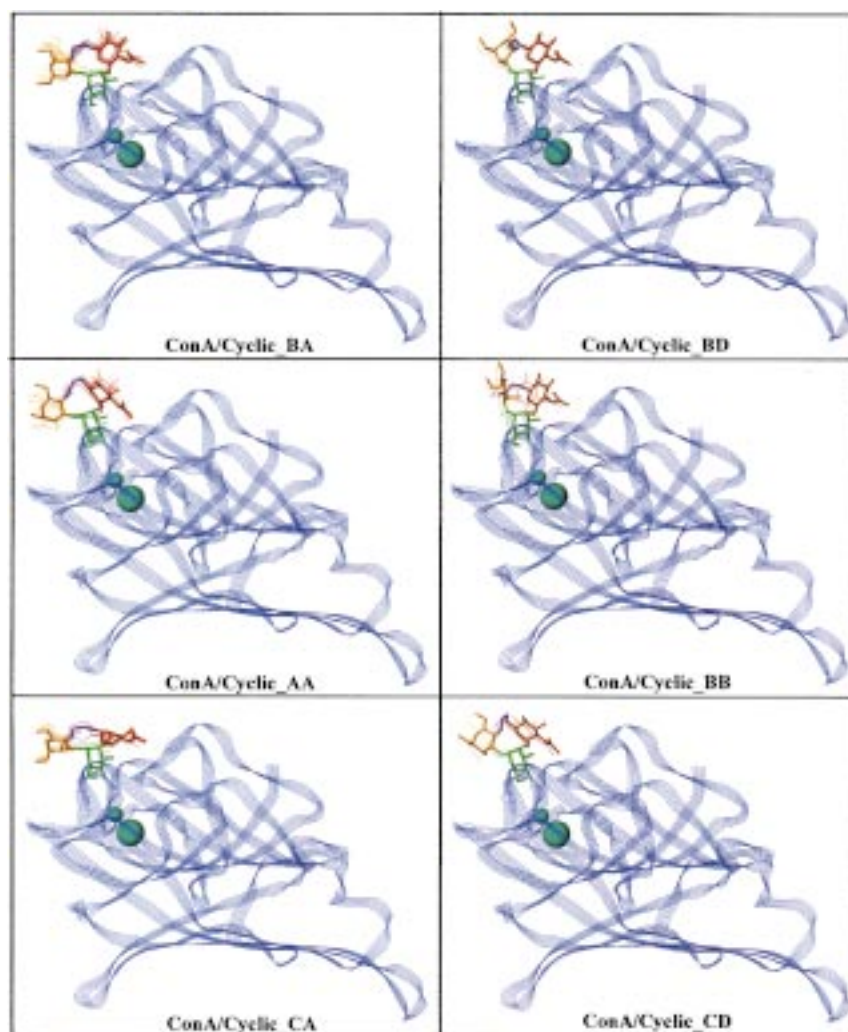


Figure 6. Graphical representation of the 20 conformers of cyclic trisaccharide **III** when interacting with ConA, distributed in six docking modes, based on the glycosidic linkage conformation. The protein is depicted by a ribbon-type representation.

Table 8. Thermodynamic data for the binding of trisaccharide **I** and **III** with ConA compared with literature data.

Compound	ΔG [kcal mol ⁻¹]	ΔH [kcal mol ⁻¹]	T ΔS [kcal mol ⁻¹]	Ref.
Man	-4.4	-5.7	-1.3	[45]
α ManOMe	-5.3	-6.6	-1.3	[46]
	-5.3	-6.8	-1.6	[45]
	-5.3	-8.2	-2.9	[47]
	-5.3	-6.8	-1.5	[48]
β GlcNAc(1 \rightarrow 2)Man	-5.2	-5.3	-0.1	[46]
α Man(1 \rightarrow 3)Man	-5.7	-10.2	-4.5	[47]
α Man(1 \rightarrow 3) α ManOMe	-5.7	-7.8	-2.0	[46]
	-6.2	-10.7	-4.5	[47]
	-6.0	-7.4	-1.4	[47]
	-5.9	-9.5	-3.6	Present work
β GlcNAc(1 \rightarrow 2) α Man(1 \rightarrow 3) α ManOMe (I)	-6.1	-4.6	1.5	Present work
4 \rightarrow 6, cyclic trisaccharide (III)	-5.8	-2.7	3.1	Present work

has a slightly more favorable energy of binding than both disaccharide constituents do. Nevertheless, the thermodynamic characteristics of the linear oligosaccharide are close to those of the β GlcNAc(1 \rightarrow 2)Man disaccharide.

It was anticipated that the conformationally constrained trisaccharide **III** can adopt a conformation required for

binding with the lectin ConA but will lose less conformational flexibility than the corresponding linear trisaccharide. Therefore, the entropic barrier associated with loss of flexibility of the cyclic oligosaccharide was expected to be smaller and should thus result in more favored binding. Indeed, the measured thermodynamic data revealed more favorable entropy of binding of compound **III**, which surprisingly is offset by a less favorable enthalpy term.

The conformational studies have shown that the introduction of the methylene acetal tether does not distort the conformation of compound **III**, but only reduces its conformational space as intended. Furthermore, the docking studies indicate that both compounds complex in similar secondary minimum energy conformations (BA) and have similar interactions with the protein surface (Figure 7).

Recently, Bundle et al.^[38] reported complexation studies of preorganized branched trisaccharides with a monoclonal

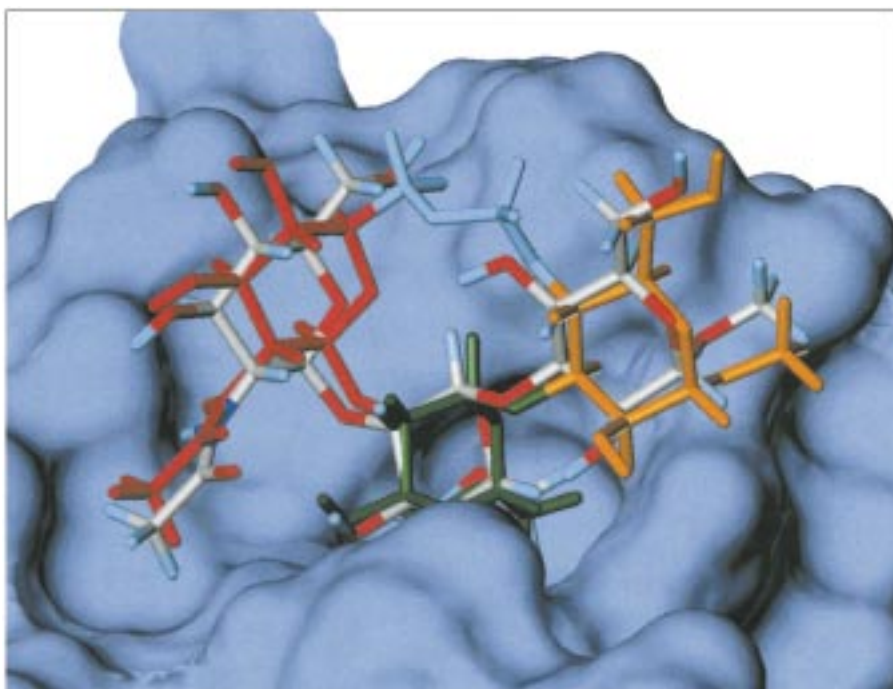


Figure 7. Comparison of the lowest energy complexes of ConA and both the linear trisaccharide **I** and the cyclic trisaccharide **III**. The solvent-accessible surface of the protein has been represented with the MOLCAD option in the SYBYL package. The linear trisaccharide **I** is colored by atom type whereas the cyclic trisaccharide **III** is colored by residue.

antibody. They found that the introduction of conformational constraints had little effect on the thermodynamic parameters of complexation and their data suggested that interresidue flexibility is not a major contributor to the weak association that characterizes oligosaccharide–protein interactions. They also proposed that the absence of large impacts on ΔH and ΔS implies that oligosaccharides display a restricted range of conformations.

The data presented in this paper show that loss of flexibility contributes significantly to the entropy of binding. Recently, Quioco and co-workers^[39] made a similar observation for the binding of linear and cyclic oligosaccharides to the maltodextrin-binding protein of *Escherichia coli*.

It is important to speculate about the origin of loss of enthalpy of binding since it may provide opportunities to

design high-affinity carbohydrate ligands.^[40] The NMR studies demonstrated that in solution both compounds populate the BA binding conformer less than 5%. Thus, upon binding a considerable unfavorable enthalpy term is introduced for this conformational change and this term may well be larger for the conformationally constrained compound explaining the less favorable enthalpy of binding. We attempted to confirm the predicted BA bound conformation of the saccharides by measuring TR-NOE's. However, despite major efforts, no TR-NOE's could be measured and the failure of these experiments is probably due to the time scale of complex dissociation and/or to the presence of a paramagnetic Mn^{2+} ion close to the sugar-binding site.

It is important to note that the calculations do not take into account enthalpy effects arising from water rearrangement and the assumption was made that the bulk solvent should have the same enthalpic effect on the complexes involving the linear and cyclic trisaccharides. However, we may speculate that the desolvation enthalpy of the cyclic compound is significantly higher than for the linear compound.

Conclusion

The synthesis of a cyclic conformationally constrained trisaccharide is described, the design of which is based on mimicking an internal hydrogen bond which is present in a docking mode of a ConA–saccharide complex.

NMR spectroscopic and molecular modeling studies have shown that the cyclic compound **III** is indeed considerably less flexible than the linear compound **I**; however, both compounds adopt mainly the conformation AA. It was anticipated that the entropy barrier of complexation of compound **III**

with ConA should be smaller because less conformational flexibility is lost during binding. Indeed, the complexation has a more favorable entropy term but surprisingly this term is offset by a smaller enthalpy contribution, and the linear and cyclic compounds have similar binding constants. Molecular modeling studies have been performed to explain the loss of enthalpy of binding, and it was predicted that both compounds are complexed in the local minimum energy conformation BA. Figure 7 displays a comparison of the lowest energy complexes of the two compounds; both have very similar interactions with the protein, and thus the small enthalpy term of complexation of the cyclic compound cannot be explained by fewer interactions with the protein.

The NMR studies have shown that in solution the BA conformation for both compounds is less than 5% populated.

Thus, a considerable amount of energy will be lost for this conformational change and it may be possible that this energy term is considerably more unfavorable for the cyclic compound. On the other hand, the observed differences of enthalpy for **III** and **I** may arise from differences in solvent reorganization.

The data presented in this paper suggest that loss of flexibility during complexation accounts for a significant entropic penalty. Further thermodynamic measurements and NMR experiments will be conducted to validate the models proposed in the present study, and these results will be important for the future design of putative high-affinity carbohydrate ligands. Cocrystallization experiments with ConA and the ligand are under way, and these experiments will confirm whether the ligands are bound in the predicted BA conformation. Other conformationally constrained saccharides that adopt the BA conformation will be prepared to study the general applicability of the observed binding data.

Experimental Section

Nomenclature: Schematic representations of the cyclic trisaccharide **I** and **III** are given in Figure 1. The three carbohydrate residues are labeled from unprimed to primed and double-primed from the ManOMe residue, by analogy to the linear compound. The relative orientation of a pair of contiguous residues about each glycosidic linkage is described by a set of two torsional angles: $\Phi_{1-3} = \text{O}-5'-\text{C}-1'-\text{O}-1'-\text{C}-3$ and $\Psi_{1-3} = \text{C}-1'-\text{O}-1'-\text{C}-3-\text{C}-4$ for the $\alpha\text{Man}(1 \rightarrow 3)\text{Man}$ linkage and $\Phi_{1-2} = \text{O}-5'-\text{C}-1'-\text{O}-1'-\text{C}-2'$ and $\Psi_{1-2} = \text{C}-1''-\text{O}-1''-\text{C}-2'-\text{C}-3'$ for the $\beta\text{GlcNAc}(1 \rightarrow 2)\text{Man}$ linkage. The orientation of the methylene acetal bridge is given by a set of five torsion angles: $\omega_1 = \text{O}-5''-\text{C}-5''-\text{C}-6''-\text{O}-6''$, $\omega_2 = \text{C}-5''-\text{C}-6''-\text{O}-6''-\text{C}-7''$, $\omega_3 = \text{C}-6''-\text{O}-6''-\text{C}-7''-\text{O}-4$, $\omega_4 = \text{O}-6''-\text{C}-7''-\text{O}-4-\text{C}-4$ and $\omega_5 = \text{C}-7''-\text{O}-4-\text{C}-4-\text{C}-5$ (Figure 3). The sign of the torsion angles is given as proposed by the Commission on Nomenclature.^[41]

Equipment: ^1H and ^{13}C NMR spectra were recorded on a Bruker AC300 spectrometer equipped with a B-ACS60 autochanger, and an Aspect 3000 off-line editing computer. The ^1H 2D-COSY^[45] spectra were recorded on a Bruker AMX400 spectrometer and an Aspect station I off-line editing computer. Chemical shifts (δ) were measured with tetramethylsilane as internal standard. Fast atom bombardment (FAB) mass spectra were recorded by means of a VG Zabspec spectrometer with *m*-nitrobenzyl alcohol as matrix.

All calculations were performed on Silicon Graphics workstations.

General methods and materials: All chemicals were purchased from Aldrich, Fluka, and Lancaster. 4 Å Molecular sieves were purchased from Avocado, activated at 300 °C for 5 h, and stored at 180 °C. Hydrogen and nitrogen (White Spot) were supplied by British Oxygen Company.

All reaction solvents were distilled prior to use: dichloromethane and 1,2-dichloroethane were distilled from P_2O_5 , acetonitrile, pyridine, and diethyl ether from CaH_2 , tetrahydrofuran (THF) from LiAlH_4 , and methanol from magnesium activated with iodine.

Chromatography was performed with Merck 7734 silica gel 60, and flash chromatography with Crosfield ES70X microspheroidal silica gel. TLC analyses were carried out on silica gel plates (Merck 1.05554 Kieselgel 60F₂₅₄). Compounds on TLC were visualized by UV light and/or by dipping in $\text{H}_2\text{SO}_4/\text{MeOH}$ (1:10 v/v/v) followed by subsequent charring at 140 °C.

Methyl (2-O-acetyl-3,4,6-tri-O-benzyl- α -D-mannopyranosyl)-(1 \rightarrow 3)-2-O-benzyl-4,6-di-O-benzylidene- α -D-mannopyranoside (3**):** A mixture of ethyl 2-O-acetyl-3,4,6-tri-O-benzyl-1-thio- α -D-mannopyranoside (**1**) (6.06 g, 11.31 mmol), methyl 2-O-benzyl-4,6-di-O-benzylidene- α -D-mannopyranoside (**2**) (3.66 g, 9.84 mmol), and 4 Å powdered molecular sieves (10 g) was stirred for 1 h in CH_2Cl_2 (120 mL). Subsequently, a solution of *N*-iodosuccinimide (120 mL, 0.1 M in ether/ CH_2Cl_2 , 1:1 v/v) and TMSOTf (0.232 mL, 1.2 mmol) were added. The mixture was stirred at room temperature for 1 h, and then neutralized with triethylamine. The solution was filtered through Celite[®], washed with $\text{MeOH}/\text{CH}_2\text{Cl}_2$, 5:95 v/v/v, and the combined filtrates were concentrated to dryness. The residue was

dissolved in CH_2Cl_2 (100 mL), and the solution was washed with $\text{Na}_2\text{S}_2\text{O}_3$ (1 M, 2 \times 100 mL) and water (100 mL). The organic layer was dried (MgSO_4), filtered, and concentrated to dryness. Purification of the crude product by column chromatography on silica gel ($\text{CH}_2\text{Cl}_2/\text{acetone}$, 99:1 v/v) afforded the desired disaccharide (**3**) as a colorless oil (8.0 g, 96 % yield); R_f (acetone/ CH_2Cl_2 , 3:97 v/v) = 0.70; $[\alpha]_{\text{D}}^{22}(\text{c}/\text{CH}_2\text{Cl}_2) = +12.1$ (CH_2Cl_2 , $c = 13.13 \text{ mg mL}^{-1}$); ^1H NMR (300 MHz, CDCl_3): $\delta = 7.52\text{--}7.15$ (m, 25H, arom H), 5.63 (s, 1H, PhCH-), 5.62 (m, 1H, H-2'), 5.32 (d, 1H, $J_{1,2} = 2.0 \text{ Hz}$, H-1'), 4.89 (d, 1H, $J_{\text{gem}} = 11.0 \text{ Hz}$, -CH₂-benzyl), 4.67 (d, 1H, $J_{1,2} = 1.5 \text{ Hz}$, H-1'), 4.77–4.60 (4d, 4H, $J_{\text{gem}} = 12.0 \text{ Hz}$, -CH₂-benzyl), 4.51–4.41 (3d, 3H, -CH₂-benzyl), 4.25 (m, 2H, H-3, H-5'), 3.98 (dd, 1H, $J_{3,2} = 3.5 \text{ Hz}$, $J_{3,4} = 9.0 \text{ Hz}$, H-3'), 3.92–3.65 (m, 8H, H-4, H-4', H-5, H-2, H-6, H-6'), 3.30 (s, 3H, -OCH₃), 2.10 (s, 3H, -CH₃ acetyl); ^{13}C NMR (75 MHz, CDCl_3): $\delta = 170.1$, (C=O), 138.7, 138.4, 137.9, 137.4 (Cq benzyl + Cq benzylidene), 128.6–126.1 (arom C), 101.1 (PhCH-), 100.6, 98.9 (C-1, C-1'), 79.1, 78.0, 77.4, 74.3, 73.2, 72.2, 68.2, 63.9 (C-2, C-3, C-4, C-5, C-2', C-3', C-4', C-5'), 75.1, 73.7, 73.5, 71.6 (-CH₂-benzyl), 69.1, 68.8 (C-6, C-6'), 54.9 (-OCH₃), 21.1 (-CH₃ acetyl); MS (FAB): m/z (%): 885 (4) [$M+K$]⁺, 869 (100) [$M+Na$]⁺; HRMS (FAB): calcd $\text{C}_{50}\text{H}_{54}\text{O}_{12}\text{Na}$ [$M+Na$]⁺ 869.35; found 869.35.

Methyl (2-O-acetyl-3,4,6-tri-O-benzyl- α -D-mannopyranosyl)-(1 \rightarrow 3)-2,6-di-O-benzyl- α -D-mannopyranoside (4**):** 4 Å molecular sieves (7 g) and sodium cyanoborohydride (4.8 g, 76.47 mmol) was added to a solution of compound **3** (6.47 g, 7.65 mmol) in dry THF (100 mL). Subsequently, a solution of HCl in ether (1 M, 99 mL) was slowly added over a period of 20 min to the mixture, which was stirred for 3 h under argon. The reaction mixture was neutralized by the addition of triethylamine, and washed with saturated NaHCO_3 (2 \times 100 mL) and water (100 mL). The organic layer was dried (MgSO_4), filtered, and concentrated under reduced pressure. The crude product was purified by column chromatography with acetone/ CH_2Cl_2 (3:97 v/v) as the eluent, and the desired disaccharide (**4**) was isolated as a colorless oil (6.03 g, 93 % yield); R_f (acetone/ CH_2Cl_2 , 2:98 v/v) = 0.10; $[\alpha]_{\text{D}}^{22}(\text{c}/\text{CH}_2\text{Cl}_2) = +27.5$ (CH_2Cl_2 , $c = 29.26 \text{ mg mL}^{-1}$); ^1H NMR (300 MHz, CDCl_3): $\delta = 7.40\text{--}7.12$ (m, 25H, arom H), 5.50 (m, 1H, H-2'), 5.37 (s, 1H, H-1'), 4.89 (d, 1H, $J_{\text{gem}} = 11.0 \text{ Hz}$, -CH₂-benzyl), 4.75–4.45 (m, 11H, $J_{\text{gem}} = 11.4 \text{ Hz}$, -CH₂-benzyl, H-1), 4.11 (dd, 1H, $J_{4,3} = 9.2 \text{ Hz}$, H-4), 3.98 (m, 3H, H-3', H-5, H-5'), 3.74 (m, 7H, H-2, H-3, H-6, H-4', H-6'), 3.33 (s, 3H, -OCH₃), 2.10 (s, 3H, -CH₃ acetyl); ^{13}C NMR (75 MHz, CDCl_3): $\delta = 170.4$, (C=O), 138.6, 138.0, 137.9 (Cq benzyl), 128.4–127.6 (arom C), 98.8, 98.7 (C-1, C-1'), 77.9, 77.5, 74.5, 71.9, 71.0, 68.8, 68.6 (C-2, C-3, C-4, C-5, C-2', C-3', C-4', C-5'), 74.9, 73.7, 72.6, 71.8, 70.8, 69.4 (-CH₂-benzyl, C-6, C-6'), 54.9 (-OCH₃), 21.1 (-CH₃ acetyl); MS (FAB): m/z (%): 887 (4) [$M+K$]⁺, 871 (100) [$M+Na$]⁺; HRMS (FAB): calcd $\text{C}_{50}\text{H}_{56}\text{O}_{12}\text{Na}$ [$M+Na$]⁺ 871.37; found 871.37.

Methyl (2-O-acetyl-3,4,6-tri-O-benzyl- α -D-mannopyranosyl)-(1 \rightarrow 3)-2,6-di-O-benzyl-4-O-methylthiomethyl- α -D-mannopyranoside (5**):** Dimethyl sulfide (5.2 mL, 70.3 mmol) was added to a cooled solution (0 °C) of **4** (5.96 g, 7.03 mmol) in dry acetonitrile (80 mL). Benzoyl peroxide (6.8 g, 28.12 mmol) was added in portions over a period of 45 min under the exclusion of light, and the mixture was stirred for 18 h and gradually allowed to reach room temperature. TLC analysis (acetone/ CH_2Cl_2 , 3:97 v/v) showed complete conversion of the starting material into the product. The solution was diluted with ethyl acetate, and washed with NaOH (1 M, 2 \times 100 mL) and brine (100 mL). The organic layer was dried (MgSO_4), filtered, and concentrated in vacuo. Purification by column chromatography on silica gel (petroleum ether 40–60/ CH_2Cl_2 , 1:1 v/v, followed by CH_2Cl_2 and acetone/ CH_2Cl_2 , 1:99 v/v) gave the compound **5** as a pale yellow foam (5.55 g, 87 % yield); R_f (acetone/ CH_2Cl_2 , 3:97 v/v) = 0.62; $[\alpha]_{\text{D}}^{22}(\text{c}/\text{CH}_2\text{Cl}_2) = +37.8$ (CH_2Cl_2 , $c = 25.73 \text{ mg mL}^{-1}$); ^1H NMR (300 MHz, CDCl_3): $\delta = 7.39\text{--}7.15$ (m, 25H, arom H), 5.35 (dd, 1H, $J_{2,1} = 1.8 \text{ Hz}$, $J_{2,3'} = 3.3 \text{ Hz}$, H-2'), 5.10 (d, 1H, H-1'), 4.89 (d, 1H, $J_{\text{gem}} = 11.0 \text{ Hz}$, -CH₂-benzyl), 4.78 (d, 1H, $J_{\text{gem}} = 11.4 \text{ Hz}$, -CH₂-benzyl), 4.72 (d, 1H, $J_{1,2} = 1.8 \text{ Hz}$, H-1), 4.67 (d, 1H, -CH₂-benzyl), 4.64–4.43 (m, 9H, -CH₂SCH₃, -CH₂-benzyl), 4.06 (dd, 1H, $J_{3,2} = 3.3 \text{ Hz}$, $J_{3,4} = 9.2 \text{ Hz}$, H-3), 3.97 (dd, 1H, $J_{3,4} = 9.2 \text{ Hz}$, H-3'), 3.88 (m, 2H, H-4, H-5'), 3.77 (m, 4H, H-2, H-4', H-6a, H-6a'), 3.68 (m, 3H, H-5, H-6b, H-6b'), 3.30 (s, 3H, -OCH₃), 2.22 (s, 3H, -CH₃ acetyl), 2.02 (s, 3H, -SCH₃); ^{13}C NMR (75 MHz, CDCl_3): $\delta = 170.3$, (C=O), 138.7, 138.4, 138.1, 137.9 (Cq benzyl), 128.5–127.6 (arom C), 99.8, 99.3 (C-1, C-1'), 77.9, 77.3, 74.5, 74.4, 72.2, 71.4, 69.1 (C-2, C-3, C-4, C-5, C-2', C-3', C-4', C-5'), 75.0, 73.5, 73.4, 73.0, 72.1, 72.0, 69.5, 69.3 (-CH₂-benzyl, -CH₂SCH₃, C-6, C-6'), 54.9 (-OCH₃), 21.2 (-CH₃ acetyl), 14.8 (-SCH₃); MS

(FAB): m/z (%): 948 (8) $[M+K]^+$, 932 (100) $[M+Na]^+$; HRMS(FAB): calcd $C_{52}H_{60}O_{12}SNa$ $[M+Na]^+$ 931.37; found 931.37.

Methyl 2,6-di-O-benzyl-3-O-(2-O-acetyl-3,4,6-tri-O-benzyl- α -D-mannopyranosyl)- α -D-mannopyranoside-*p*-methoxyphenyl 3',4'-di-O-benzyl-2'-deoxy-2'-phthalimido- β -D-glucopyranoside-4,6''-methylidene acetal (7): A mixture of **5** (5.1 g, 5.62 mmol), *p*-methoxyphenyl 3,4-di-O-benzyl-2-deoxy-2-phthalimido- β -D-glucopyranoside (**6**) (2.90 g, 4.88 mmol) and powdered molecular sieves (8 g) was stirred for 1 h in a mixture of THF and 1,2-dichloroethane (1:1 v/v, 100 mL) under argon. The solution was cooled to 0 °C. *N*-iodosuccinimide (1.35 g, 6 mmol) was dissolved in a mixture of THF and 1,2-dichloroethane (60 mL, 1:1 v/v). Trifluoromethanesulfonic acid (54 μ L, 0.6 mmol) was then added and the solution stirred for further 30 s. The resulting mixture (0.1M, 58.7 mL) was added quickly to the initial solution which was then stirred for 30 min at 0 °C. TLC analysis indicated the conversion of the starting material into a major product. The reaction mixture was neutralized by the addition of triethylamine and filtered through Celite. The resulting solution was diluted with CH_2Cl_2 (200 mL) and washed with $Na_2S_2O_3$ (2 \times 100 mL), $NaHCO_3$ (100 mL) and brine (100 mL). The organic layer was dried ($MgSO_4$), filtered, and concentrated to dryness. Purification of the crude product by column chromatography on silica gel (CH_2Cl_2 /acetone, 98:2 v/v) afforded the trisaccharide **7** as a colorless oil (5.39 g, 76% yield); R_f (acetone/ CH_2Cl_2 , 4:96 v/v) = 0.66; $[\alpha]_{D}^{25} = +44.4$ (CH_2Cl_2 , $c = 26.8$ mg mL $^{-1}$); 1H NMR (300 MHz, $CDCl_3$): $\delta = 7.65$ (brs, 4H, arom H -Pht), 7.38–6.85 (m, 35H, arom H), 6.80, 6.65 (2 m, 4H, arom H -MP), 5.59 (d, 1H, $J_{1',2'} = 8.1$ Hz, H-1'), 5.56 (dd, 1H, $J_{2',1'} = 1.8$ Hz, $J_{2',3'} = 3.3$ Hz, H-2'), 5.21 (d, 1H, H-1'), 5.02 (d, 1H, $J_{gem} = 6.3$ Hz, $-OCH_2O-$), 4.94–4.42 (m, 16H, H-1, $-OCH_2O-$, $-CH_2-$ benzyl), 4.40 (m, 1H, H-2''), 4.02 (dd, 1H, $J_{3,2} = 2.6$ Hz, $J_{3,4} = 9.6$ Hz, H-3), 4.38–3.53 (m, 15H, H-2, H-4, H-5, H-6, H-3', H-4', H-5', H-6', H-3'', H-4'', H-5'', H-6''), 3.62 (s, 3H, $-OCH_3$ -MP), 3.25 (s, 3H, $-OCH_3$), 2.10 (s, 3H, $-CH_3$ acetyl); ^{13}C NMR (75 MHz, $CDCl_3$): $\delta = 170.0$ (C=O), 151.0 (Cq -MP), 138.0 (Cq benzyl), 133.7, 123.3 (arom C -Pht), 131.6 (Cq -Pht), 128.5–127.4 (arom C), 118.6, 114.4 (arom C -MP), 100.1, 98.8, 97.7 (C-1, C-1'), 97.8 ($-OCH_2O-$), 79.6, 79.1, 77.8, 77.5, 74.3, 74.1, 72.2 (C-2, C-3, C-4, C-5, C-2', C-3', C-4', C-5'), 74.8, 73.4, 73.0, 72.1, 71.9, 69.8, 69.2, 67.5 ($-CH_2-$ benzyl, C-6, C-6'), 64.1 (C-6''), 55.9, 55.7, 54.8 ($-OCH_3$ -MP, $-OCH_3$, C-2''), 21.1 ($-CH_3$ acetyl); MS (FAB): m/z (%): 1478 (100) $[M+Na]^+$; HRMS (FAB): calcd $C_{86}H_{89}NO_{20}Na$ $[M+Na]^+$ 1478.59; found 1478.59.

Methyl 2,6-di-O-benzyl-3-O-(3,4,6-tri-O-benzyl- α -D-mannopyranosyl)- α -D-mannopyranoside-3',4'-di-O-benzyl-2'-deoxy-2'-phthalimido- β -D-glucopyranoside-4,6''-methylidene acetal (9): Potassium *tert*-butoxide (0.412 g, 3.67 mmol) was added to a solution of trisaccharide **7** (5.34 g, 3.67 mmol) in methanol (50 mL). The resulting mixture was stirred at room temperature under argon. After 4 h, TLC analysis (acetone/ CH_2Cl_2 , 3:97 v/v) showed the complete conversion of the starting material. The reaction mixture was neutralized with Dowex-50WX8-[H $^+$] and filtered, and the filtrate concentrated to dryness in vacuo. The crude compound **8** was used without further purification. Compound **8** was dissolved in a mixture of toluene/acetonitrile/water (60 mL, 1:4:1 v/v/v), and cerium ammonium nitrate (6.04 g, 11.01 mmol) was added. The mixture was stirred for 4 h at room temperature under the exclusion of light, after which time the solution was diluted with ethyl acetate. The organic layer was washed with saturated $NaHCO_3$ (2 \times 75 mL) and brine (75 mL), dried ($MgSO_4$), and filtered, and the filtrate concentrated under reduced pressure. The crude product was purified by column chromatography on silica gel with acetone/ CH_2Cl_2 (4:96 v/v) as the eluent. The trisaccharide **9** was obtained as a pale yellow oil (2.16 g, 45% yield); R_f (acetone/ CH_2Cl_2 , 5:95 v/v) = 0.20; $[\alpha]_{D}^{25} = +29.8$ (CH_2Cl_2 , $c = 20.8$ mg mL $^{-1}$); 1H NMR (300 MHz, $CDCl_3$): $\delta = 7.80$ –7.60 (4H, m, arom H -Pht), 7.41–6.88 (m, 35H, arom H), 5.32 (d, 1H, $J_{1',2'} = 1.1$ Hz, H-1'), 5.25 (d, 1H, $J_{1',2'} = 8.5$ Hz, H-1''), 4.85 (2d, 2H, $J_{gem} = 11.0$ Hz, $-CH_2-$ benzyl), 4.70 (d, 1H, $J_{1,2} = 1.4$ Hz, H-1), 4.81–4.39 (m, 15H, $-OCH_2O-$, $-CH_2-$ benzyl, H-3''), 4.27 (brs, 1H, H-2'), 4.13 (dd, 1H, $J_{2',3'} = 10.7$ Hz, H-2''), 4.09 (m, 1H, H-3), 4.01–3.54 (m, 14H, H-2, H-4, H-5, H-6, H-3', H-4', H-5', H-6', H-3'', H-4'', H-5'', H-6''), 3.31 (s, 3H, $-OCH_3$); ^{13}C NMR (75 MHz, $CDCl_3$): $\delta = 168.2$ (C=O), 138.7, 138.4, 138.3, 138.2, 138.0 (Cq benzyl), 133.7, 123.2 (arom C -Pht), 131.8 (Cq -Pht), 128.5–126.6 (arom C), 100.7, 98.6, 92.9 (C-1, C-1', C-1''), 97.6 ($-OCH_2O-$), 79.7, 79.3, 79.2, 78.0, 76.3, 75.7, 74.6, 74.5, 71.7, 71.5, 68.3 (C-2, C-3, C-4, C-5, C-2', C-3', C-4', C-5', C-3'', C-4'', C-5'', H-6, H-6'), 74.8, 74.6, 73.4, 71.9, 69.5, 69.3 ($-CH_2-$ benzyl, C-6, C-6'), 57.7, 54.9 ($-OCH_3$, C-2''); MS (FAB): m/z (%): 1346 (3)

$[M+K]^+$, 1330 (100) $[M+Na]^+$; MS (FAB): calcd $C_{77}H_{81}NO_{18}Na$ $[M+Na]^+$ 1330.54; found 1330.53.

Methyl 2,6-di-O-benzyl-3-O-(3,4,6-tri-O-benzyl- α -D-mannopyranosyl)- α -D-mannopyranoside-trichloroacetimidate 3',4'-di-O-benzyl-2'-deoxy-2'-phthalimido- β -D-glucopyranoside-4,6''-methylidene acetal (10): Trichloroacetonitrile (0.782 mL, 7.80 mmol) and 1,8-diazabicyclo[5.4.0]undec-7-ene (19.5 μ L, 0.13 mmol) were added to a solution of **9** (1.7 g, 1.3 mmol) in CH_2Cl_2 (30 mL) and the reaction mixture was stirred under argon. After 20 min the TLC analysis (CH_2Cl_2 /acetone, 95:5 v/v) showed almost complete conversion of the starting material into the product. The mixture was concentrated in vacuo and the oily residue was applied onto a column of silica gel and eluted with acetone/ CH_2Cl_2 (1:99 v/v). Concentration of the appropriate fractions gave **10** as a white foam (1.22 g, 65% yield); R_f (acetone/ CH_2Cl_2 , 5:95 v/v) = 0.50; $[\alpha]_{D}^{25} = +53.3$ (CH_2Cl_2 , $c = 1$ 9.6 mg mL $^{-1}$); 1H NMR (300 MHz, $CDCl_3$): $\delta = 8.41$ (s, 1H, C=NH), 7.65 (brs, 4H, arom H -Pht), 7.40–6.80 (m, 35H, arom H), 6.37 (d, 1H, $J_{1',2'} = 8.5$ Hz, H-1'), 5.15 (d, 1H, $J_{1',2'} = 1.1$ Hz, H-1''), 4.87 (d, 1H, $J_{gem} = 11.4$ Hz, $-CH_2-$ benzyl), 4.85 (d, 1H, $J_{gem} = 11.0$ Hz, $-CH_2-$ benzyl), 4.82–4.35 (m, 17H, $-OCH_2O-$, $-CH_2-$ benzyl, H-1, H-2'', H-3''), 4.15 (brs, 1H, H-2'), 4.03 (dd, 1H, $J_{3,2} = 3.3$ Hz, $J_{3,4} = 9.2$ Hz, H-3), 3.98–3.52 (m, 14H, H-2, H-4, H-5, H-6, H-3', H-4', H-5', H-6', H-4'', H-5'', H-6''), 3.31 (s, 3H, $-OCH_3$), 3.10 (brs, 1H, $-OH$); ^{13}C NMR (75 MHz, $CDCl_3$): $\delta = 168.0$ (C=O), 160.9 (Cq imidate), 138.7, 137.9 (Cq benzyl), 133.8, 123.3 (arom C -Pht), 131.5 (Cq -Pht), 128.5–127.4 (arom C), 102.1, 98.3, 94.0 (C-1, C-1', C-1''), 97.6 ($-OCH_2O-$), 80.2, 79.5, 78.9, 77.6, 75.7, 74.8, 74.6, 71.3, 68.4 (C-2, C-3, C-4, C-5, C-2', C-3', C-4', C-5', C-3'', C-4'', C-5''), 74.9, 74.7, 73.5, 73.2, 72.1, 69.7, 69.5, 67.1 ($-CH_2-$ benzyl, C-6, C-6', C-6''), 54.8 ($-OCH_3$, C-2''); MS (FAB): m/z (%): 1473 (73) $[M+Na+3 \times ^{35}Cl]^+$, 1476 (100), $[M+Na+2 \times ^{35}Cl+1 \times ^{37}Cl]^+$, 1479 (32) $[M+Na+1 \times ^{35}Cl+2 \times ^{37}Cl]^+$; HRMS (FAB): calcd $C_{79}H_{81}N_2O_{18}^{35}Cl_3Na$ $[M+Na]^+$ 1473.44; found 1473.44; calcd $C_{79}H_{81}N_2O_{18}^{35}Cl_2^{37}ClNa$ $[M+Na]^+$ 1475.44; found 1475.44; calcd $C_{79}H_{81}N_2O_{18}^{35}Cl^37Cl_2Na$ $[M+Na]^+$ 1477.44; found 1477.44.

Methyl (3,4-di-O-benzyl-2-deoxy-2-phthalimido- β -D-glucopyranosyl)-(1-2)-(3,4,6-tri-O-benzyl- α -D-mannopyranosyl)-(1-3)-2,6-di-O-benzyl- α -D-mannopyranoside-4,6''-methylidene acetal (11): A mixture of **10** (1.22 g, 0.84 mmol) and 4 Å powdered molecular sieves (1 g) was stirred for 30 min in CH_2Cl_2 (50 mL) under argon. The solution was cooled to –20 °C and trimethylsilyl trifluoromethanesulfonate (8 μ L, 0.042 mmol) was added and the reaction mixture was stirred for 10 min. The reaction mixture was quenched by the addition of triethylamine and filtered through Celite; the filtrate was diluted with CH_2Cl_2 , and washed with $NaHCO_3$ (2 \times 50 mL) and water (50 mL). The organic layer was dried ($MgSO_4$), filtered, and concentrated to dryness. Purification of the residue by column chromatography on silica gel (CH_2Cl_2 /acetone, 98:2 v/v) afforded the cyclic trisaccharide **11** as a colorless oil (891.8 mg, 82% yield); R_f (CH_2Cl_2 /acetone, 96:4 v/v) = 0.78; $[\alpha]_{D}^{25} = +42.1$ (CH_2Cl_2 , $c = 20.53$ mg mL $^{-1}$); 1H NMR (300 MHz, $CDCl_3$): $\delta = 7.52$ (brs, 4H, arom H -Pht), 7.41–6.80 (m, 35H, arom H), 5.75 (2d, 2H, $J_{1',2'} = 7.7$ Hz, H-1', H-1''), 5.06 (d, 1H, $J_{gem} = 4.0$ Hz, $-OCH_2O-$), 4.88 (d, 1H, $J_{gem} = 11.0$ Hz, $-CH_2-$ benzyl), 4.67 (d, 1H, $J_{1,2} = 1.5$ Hz, H-1), 4.83–4.23 (m, 15H, $-OCH_2O-$, $-CH_2-$ benzyl, H-2'', H-2'), 4.15 (d, 1H, $J_{gem} = 10.7$ Hz, $-CH_2-$ benzyl), 4.11 (dd, 1H, $J_{3,2} = 2.9$ Hz, H-3), 3.99 (2dd, 2H, $J_{4,3} = 9.9$ Hz, H-4, H-4''), 3.82–3.44 (m, 13H, H-2, H-5, H-6, H-3', H-4', H-5', H-6', H-3'', H-4'', H-5'', H-6''), 3.25 (s, 3H, $-OCH_3$); ^{13}C NMR (75 MHz, $CDCl_3$): $\delta = 167.9$ (C=O), 139.1, 138.4, 138.1, 137.9, 137.7 (Cq benzyl), 133.4, 123.1 (arom C -Pht), 131.6 (Cq -Pht), 128.5–126.8 (arom C), 100.0, 99.0, 94.5 (C-1, C-1', C-1''), 96.9 ($-OCH_2O-$), 79.2, 78.9, 77.2, 76.8, 76.0, 75.3, 74.5, 72.0, 71.8, 71.3 (C-2, C-3, C-4, C-5, C-2', C-3', C-4', C-5', C-3'', C-4'', C-5''), 74.9, 74.3, 73.5, 73.2, 72.5, 72.3, 69.1, 68.8, 66.2 ($-CH_2-$ benzyl, C-6, C-6', C-6''), 54.7, 53.8 (C-2', $-OCH_3$); MS (FAB): m/z (%): 1328 (8) $[M+K]^+$, 1312 (100) $[M+Na]^+$; HRMS (FAB): calcd $C_{77}H_{79}NO_{17}Na$ $[M+Na]^+$ 1312.52; found 1312.52.

Methyl (3,4-di-O-benzyl-2-acetimidido-2-deoxy- β -D-glucopyranosyl)-(1-2)-(3,4,6-tri-O-benzyl- α -D-mannopyranosyl)-(1-3)-2,6-di-O-benzyl- α -D-mannopyranoside-4,6''-methylidene acetal (12): Hydrazine monohydrate (1.78 mL, 36.69 mmol) was added to a solution of **11** (945.8 mg, 0.733 mmol) in EtOH (10 mL) and the reaction mixture was heated under reflux for 18 h. TLC analysis with ninhydrin showed complete conversion of the starting material into an amino-containing intermediate (R_f (acetone/ CH_2Cl_2 , 4:96 v/v) = 0.10). The solvent was removed in vacuo and the residue coevaporated with toluene. The amine thus obtained was subsequently dissolved in a mixture of pyridine (10 mL) and acetic

anhydride (10 mL) and the solution was stirred at room temperature for 4 h. The mixture was then concentrated and coevaporated with toluene (3 × 20 mL), ethanol (2 × 20 mL) and CH₂Cl₂ (2 × 20 mL). Purification of the crude product by column chromatography on silica gel (CH₂Cl₂/acetone, 97:3 v/v) gave the title compound **12** (563.4 mg, 64% yield) as a colorless oil; *R*_f (acetone/CH₂Cl₂, 4:96 v/v) = 0.23; [α]_D²⁵ = +31.2 (CH₂Cl₂, *c* = 16.93 mg mL⁻¹); ¹H NMR (300 MHz, CDCl₃): δ = 7.45–7.11 (m, 35H, arom H), 5.43 (d, 1H, *J*_{NH,2'} = 6.3 Hz, NH), 5.39 (s, 1H, H-1'), 5.22 (d, 1H, *J*_{1',2'} = 8.8 Hz, H-1''), 4.91, 4.90, 4.85 (3d, 3H, *J*_{gem} = 11.0 Hz, -CH₂-benzyl), 4.79–4.48 (m, 15H, -OCH₂O-, -CH₂-benzyl, H-1, H-3''), 4.22 (s, 1H, H-2'), 4.08–3.97 (m, 2H, H-3, H-4), 3.88–3.48 (m, 13H, H-2, H-5, H-6, H-3', H-4', H-5', H-6', H-4'', H-5'', H-6''), 3.27 (s, 3H, -OCH₃), 2.91–2.80 (m, 1H, H-2''); ¹³C NMR (75 MHz, CDCl₃): δ = 171.0 (C=O), 139.3, 138.5, 138.3, 138.1, 137.8 (C_q benzyl), 129.0–127.5 (arom C), 102.9, 98.6, 96.3 (C-1, C-1', C-1''), 97.2 (-OCH₂O-), 79.0, 78.2, 78.0, 77.5, 76.8, 76.3, 75.9, 74.3, 72.6, 72.1, 70.5 (C-2, C-3, C-4, C-5, C-2', C-3', C-4', C-5'), 75.1, 74.8, 74.5, 73.6, 72.6, 69.3, 69.1, 66.1 (-CH₂-benzyl, C-6, C-6', C-6''), 56.2, 54.8 (C-2'', -OCH₃), 23.5 (-CH₃ acetyl); MS (FAB): *m/z* (%): 1240 (5) [M+K]⁺, 1224 (100) [M+Na]⁺; HRMS (FAB): calcd C₇₁H₇₉NO₁₆Na [M+Na]⁺ 1224.53; found 1224.53.

Methyl (2-acetimido-2-deoxy-β-D-glucopyranosyl)-(1 → 2)-(α-D-mannopyranosyl)-(1 → 3)-α-D-mannopyranoside-4,6''-methylidene acetal (III): Compound **12** (536.6 mg, 0.447 mmol) in ethanol (10 mL) was hydrogenated (H₂, 54 mg Pd(OAc)₂) for 18 h. The mixture was filtered through Celite and concentrated. The cyclic trisaccharide **III** was obtained as a white solid (230 mg, 90% yield); *R*_f (MeOH/CH₂Cl₂, 20:80 v/v) = 0.05; [α]_D²⁵ = +34.7 (MeOH, *c* = 3.4 mg mL⁻¹); ¹H NMR (400 MHz, D₂O): δ = 5.68 (d, 1H, *J*_{1',2'} = 1.3 Hz, H-1'), 5.15, 5.02 (2d, 2H, *J*_{gem} = 5.1 Hz, -OCH₂O-), 4.95 (d, 1H, *J*_{1',2'} = 8.4 Hz, H-1''), 4.83 (d, 1H, *J*_{1,2} = 1.5 Hz, H-1), 4.37 (dd, 1H, *J*_{2,3} = 3.9 Hz, H-2'), 4.20–3.92 (m, 8H, H-2, H-3, H-6a, H-3', H-6a', H-2'', H-6a'', H-6b''), 3.90–3.56 (m, 9H, H-4, H-5, H-6b, H-4', H-5', H-6b', H-3'', H-4'', H-5''), 3.49 (s, 3H, -OCH₃), 2.13 (s, 3H, -CH₃ acetyl); ¹³C NMR (100 MHz, D₂O): δ = 177.5 (C=O), 103.1 (*J*_{C1,H1} = 173.5 Hz, C-1), 102.0 (*J*_{C1',H1'} = 173.3 Hz, C-1'), 100.4 (-OCH₂O-), 99.6 (*J*_{C1'',H1''} = 166.4 Hz, C-1''), 78.7, 77.7, 76.9, 76.4, 75.7, 75.0, 74.4, 72.5, 71.8, 71.6, 69.3 (C-2, C-3, C-4, C-5, C-2', C-3', C-4', C-5'), 70.4 (C-6''), 63.4, 62.7 (C-6, C-6'), 57.3 (-OCH₃), 56.6 (C-2''), 24.8 (-CH₃ acetyl); MS (FAB): *m/z* (%): 616 (7) [M+2 × Na]⁺, 594 (100) [M+Na]⁺; MS (FAB): calcd C₂₂H₃₇NO₁₆Na [M+Na]⁺ 594.20; found 594.20.

Microcalorimetry: Isothermal titration calorimetry (ITC) experiments to measure the binding of saccharides to concanavalin A were done at 25 °C by means of a Microcal MCS titration microcalorimeter following standard instrumental procedures^[42] with a 250 μL injection syringe and 400 rpm stirring. Concanavalin A (Sigma) was used without further purification and was dissolved in a buffer (0.1 M Tris, 0.5 M NaCl, 1 mM MnCl₂, 1 mM CaCl₂, pH 7.0) and degassed gently immediately before use. Saccharide ligands were dissolved in the same buffer. Protein concentrations in the ITC cell were determined from UV absorbance measurements at 280 nm with the molar extinction coefficient ε₂₈₀ = 33 000 (ConA). A typical binding experiment involved 25 × 10 μL injections of ligand solution (typically around 10 mM concentration) into the ITC cell (ca. 1.3 mL active volume) containing protein (0.1–0.5 mM). Control experiments were performed under identical conditions by injection of ligand into buffer alone (to correct for heats of ligand dilution) and injection of buffer into the protein mix (to correct for heats of dilution of the protein). Integrated heat effects, after correction for heats of dilution, were analyzed by nonlinear regression in terms of a simple single-site binding model using the standard Microcal ORIGIN software package. For each thermal titration curve this yields estimates of the apparent number of binding sites (*N*) on the protein, the binding constant (*K*, M⁻¹) and the enthalpy of binding (Δ*H*, kcal mol⁻¹). In cases of weak ligand binding the titration curve is too gradual to allow unambiguous estimation of *N*, and in such cases the stoichiometry was fixed at *N* = 1 for regression fits. Other thermodynamic quantities were calculated with the standard expression Δ*G*^o = -*RT* ln *K* = Δ*H*^o - *T*Δ*S*^o.

Molecular modeling:

Starting models for the oligosaccharides and for ConA: The trisaccharide βGlcNAc(1 → 2)αMan(1 → 3)Man was constructed with the monosaccharides obtained from a database of three-dimensional structures.^[43] All subsequent calculations were performed by SYBYL software. Cyclization was performed through a systematic search around the four torsion angles of the glycosidic linkage, while a short distance was imposed between the

atom O-4 and O-6''. The solution with the best energy was taken as a starting point for the cyclic compound. The coordinates of concanavalin A were taken from the 2.0 Å resolution crystal structure of the ConA-mannose complex.^[35] Four conserved water molecules, which are involved in the coordination of the structural cations, were incorporated into the model. All hydrogen atoms were added and their position optimized with the Tripos force field.^[44]

Systematic conformational search for the trisaccharides: For the linear trisaccharide, a four-dimensional systematic search was performed by rotating the Φ and Ψ angles of the two glycosidic linkages by 10° steps. The SEARCH procedure of the SYBYL software was used for this purpose together with energy parameters appropriate for carbohydrates.^[37] In order to avoid limitation of conformational space due to steric conflicts in the rigid-residue approach, the hydroxyl hydrogens were omitted and the hydroxymethyl groups at C-6 were replaced by methyl groups. In order to limit the computation time needed, all conformations with penetration of van der Waals spheres larger than 40% were rejected prior to any energy calculations.

A systematic search of the possible conformations of the 13-membered ring has been performed on the cyclic trisaccharide. In the 13-membered ring of this cyclic trisaccharide, nine torsion angles could be rotated, one of which was used as a ring-closure bond. An eight-dimensional systematic conformational search was performed by rotating the Φ and Ψ torsion angles of the two glycosidic linkages as well as the torsion angles of the methylene acetal bridge by 10° steps, except for ω₃, which corresponds to the ring-closure bond.

In order to establish the correct stereochemistry at the ring-closure point and to relieve small steric conflicts, each of the resulting conformations of the cyclic trisaccharide was submitted to several steps of energy minimization. The hydroxyl atoms were restored, and the charges and atom types specially defined for carbohydrate parameterization^[37] were used. The first cycles included constraints on the torsion angles. The final optimization was run with a termination gradient of 0.05 rms with no constraints. The structures obtained after the systematic search were checked for the puckering of the pyranose rings and chirality of carbon atoms.

A family analysis method^[8] was used to identify groups of conformations. In this approach, a family algorithm was used which concludes that an object belongs to a group if there is only a single-step change to at least one of the objects in the group. For this purpose, the torsion angles of both the βGlcNAc(1 → 2)Man and the αMan(1 → 3)Man glycosidic linkage were used as selection criteria and the step limit was fixed at 30°.

Docking in the binding site of ConA: The lowest energy conformation of each family of compound **I** and each of the low-energy conformations of compound **III**, in an energy window of 10 kcal mol⁻¹, were used as starting structures to be docked in the binding site of ConA. This was performed by superimposing the central mannose unit of the cyclic trisaccharide onto the sugar ring in the ConA-mannose complex.^[35] The hydroxyl groups were oriented in order to create the appropriate hydrogen network between the mannose residue and the amino acids of the binding site. Each of these ConA-trisaccharide complexes was optimized by means of the appropriate energy parameters.^[37] Two shells of amino acids were considered for the optimization cycle. A 10 Å shell around the binding site (33 amino acids as well as the water molecules and cations) was taken into account for the energy calculations. A 4 Å shell containing the 15 amino acids closest to the carbohydrate (Tyr¹², Asn¹⁴, Thr⁹⁷, Gly⁹⁸, Leu⁹⁹, Tyr¹⁰⁰, Ser¹⁶⁸, Ala²⁰⁷, Asp²⁰⁸, Gly²²⁴, Ser²²⁵, Thr²²⁶, Gly²²⁷, Arg²²⁸, and Leu²²⁹) was defined as the hot region to be optimized. In the first optimization cycles, only the cyclic trisaccharide and the side chains of these 15 amino acids were allowed to optimize. In the second step, the backbone of these amino acids was also optimized.

Conformational analysis by NMR spectroscopy: NMR experiments were recorded on a Bruker DRX500 spectrometer, with an approximately 5 mg mL⁻¹ solution of the trisaccharides in D₂O at 299 K. Chemical shifts are reported in ppm, with the residual HDO signal (δ = 4.72) and external TMS (δ = 0) as references. The double quantum filtered COSY spectrum was recorded with a data matrix of 256 × 1 k to digitize a spectral width of 2000 Hz. 16 scans were used with a relaxation delay of 1 s. The 2D-TOCSY experiment was performed with a data matrix of 256 × 2 k to digitize a spectral width of 2000 Hz; 16 scans were used per increment with a relaxation delay of 2 s, and MLEV 17 with 100 ms isotropic mixing time. The one-bond proton-carbon correlation experiment was collected by means of the gradient-enhanced HMQC sequence. A data matrix of 256 ×

1 k was used to digitize a spectral width of 2000 Hz in F2 and 10000 Hz in F1. 4 scans were used per increment with a relaxation delay of 1 s and a delay corresponding to a J value of 145 Hz. ^{13}C decoupling was achieved by the WALTZ scheme.

The 2D-HMQC-TOCSY experiment was conducted with 80 ms mixing time (MLEV 17). The same conditions as for the HMQC were employed. HMBC experiments were performed with the gradient-enhanced sequence with a data matrix of $256 \times 2\text{ k}$ to digitize a spectral width of 2000×15000 Hz. Eight scans were acquired per increment with a delay of 65 ms for evolution of long-range couplings. NOESY experiments were recorded with mixing times of 100, 200, 300, and 400 ms. ROESY experiments used mixing times of 100, 200, 300, and 400 ms. The rf carrier frequency was set at $\delta = 6.0$, and the spin locking field was 3.0 kHz. Good linearity of the build-up curves was observed up to 250 ms (NOESY) and 300 ms (ROESY). Estimated errors are smaller than 10%. Assuming that the motion of two interacting protons can be described by a monoexponential autocorrelation function, the corresponding cross-relaxation rates are given in Equations (1) and (2).

$$\sigma_{\text{NOESY}} = (k_2/10^6)[6J(2\omega) - J(0)] \quad (1)$$

$$\sigma_{\text{ROESY}} = (k_2/10^6)[2J(0) + 3J(\omega)] \quad (2)$$

Cross-relaxation rates were estimated from the build-up courses by extrapolation at zero mixing time.^[31,32] Effective correlation times and, thus, interproton distances, for selected proton pairs may be obtained from $\sigma_{\text{NOESY}}/\sigma_{\text{ROESY}}$ ratios, since they only depend on τ_c . Developing the spectral density functions, $J(n\omega)$, as a function of the correlation time, τ_c , and of the spectrometer frequency, ω_0 , we obtain Equation (3), which is a quartic

$$\sigma_{\text{ROESY}}/\sigma_{\text{NOESY}} = (5 + 22\omega_0^2\tau_c^2 + 8\omega_0^4\tau_c^4)/(5 + \omega_0^2\tau_c^2 - 4\omega_0^4\tau_c^4) \quad (3)$$

equation in τ_c , which can be easily solved. It should be stressed that the assumption made here does not require equal mobility between different proton pairs, as in a rigid molecule. Therefore, it is possible to obtain internuclear distances r (geometrical parameter) and local correlation times (dynamic parameter) for any pair of protons.^[33] This approach reduces the intrinsic error resulting from the use of an internal reference (as in the isolated-spin-pair approximation).

Acknowledgment

The research is supported by TMR Marie Curie Research Grant Financial (N.N.), by DGICYT (project PB96-0833) (J.J.B.), and by Pfizer (N.A.). SIdI-UAM provided facilities throughout this work (A.P.).

- [1] a) J. M. Rini, *Annu. Rev. Biophys. Biomol. Struct.* **1995**, *24*, 551–577; b) N. K. Vyas, *Curr. Opin. Struct. Biol.* **1991**, *1*, 732–740; c) W. I. Weis, K. Drickamer, *Annu. Rev. Biochem.* **1996**, *65*, 441–473; d) K. Drickamer, *Structure* **1997**, *5*, 465–472; e) H. Lis, N. Sharon, *Chem. Rev.* **1998**, *98*, 637–674.
- [2] E. J. Toone, *Curr. Opin. Struct. Biol.* **1994**, *4*, 719–728.
- [3] R. U. Lemieux, L. T. J. Delbaere, H. Beierbeck, U. Spohr, *Ciba Found. Symp.* **1991**, *158*, 231–238.
- [4] J. P. Carver, *Pure Appl. Chem.* **1993**, *65*, 763–770.
- [5] Y. Bourne, P. Rougé, C. Cambillau, *J. Biol. Chem.* **1992**, *267*, 197–204; b) Y. Bourne, J. Mazurier, D. Legrand, P. Rougé, J. Montreuil, G. Spik, C. Cambillau, *Structure* **1994**, *2*, 209–219.
- [6] Y. Bourne, B. Bolgiano, D. I. Liao, G. Strecker, P. Cantau, O. Herzberg, T. Feizi, C. Cambillau, *Nat. Struct. Biol.* **1994**, *1*, 863–870.
- [7] a) A. Imberty, Y. Bourne, C. Cambillau, P. Rougé, S. Pérez, *Adv. Biophys. Chem.* **1993**, *3*, 71–117; b) A. Imberty, *Curr. Opin. Struct. Biol.* **1997**, *7*, 617–623.
- [8] A. Imberty, S. Pérez, *Glycobiology* **1994**, *4*, 351–366.
- [9] N. Navarre, A. H. van Oijen, G. J. Boons, *Tetrahedron Lett.* **1997**, *38*, 2023–2026.
- [10] T. Peters, *Liebigs Ann. Chem.* **1991**, *2*, 135–141.
- [11] a) Y. Kondo, K. Noumi, S. Kitagawa, S. Hirano, *Carbohydr. Res.* **1983**, *123*, 157–159; b) H. B. Borén, P. J. Garegg, N. H. Wallim, *Acta. Chem. Scand.* **1972**, *26*, 1082–1086.
- [12] T. Nakano, Y. Ito, T. Ogawa, *Carbohydr. Res.* **1993**, *243*, 43–69.
- [13] G. H. Veeneman, S. H. van Leeuwen, J. H. van Boom, *Tetrahedron Lett.* **1990**, *31*, 1331–1334.
- [14] P. J. Garegg, H. Hultberg, S. Wallim, *Carbohydr. Res.* **1982**, *108*, 97–101.
- [15] P. J. L. M. Quaedflieg, C. M. Timmers, V. E. Kal, G. A. van der Marel, E. Kuyl-Yeheskiely, J. H. van Boom, *Tetrahedron Lett.* **1992**, *33*, 3081–3084.
- [16] R. R. Schmidt, *Angew. Chem.* **1986**, *98*, 213–236; *Angew. Chem. Int. Ed. Engl.* **1986**, *25*, 212–235.
- [17] T. Fukuyama, A. A. Laird, L. M. Hotchkiss, *Tetrahedron Lett.* **1985**, *26*, 6291–6292.
- [18] J. Alais, A. Veyrieres, *Carbohydr. Res.* **1990**, *207*, 11–31.
- [19] T. Sokolowski, T. Peters, S. Pérez, A. Imberty, *J. Mol. Graph.* **1997**, *15*, 37–42.
- [20] N. L. Allinger, Y. H. Yuh, J. H. Lii, *J. Am. Chem. Soc.* **1989**, *111*, 8551–8566.
- [21] a) J. R. Brisson, J. P. Carver, *Biochemistry* **1983**, *22*, 3671–3689; b) H. Paulsen, T. Peters, V. Sinnwell, R. Leubuh, B. Meyer, *Liebigs Ann. Chem.* **1985**, 489–509; c) S. W. Homans, R. A. Dwek, T. W. Rademacher, *Biochemistry* **1987**, *26*, 6553–6560.
- [22] A. Imberty, V. Tran, S. Pérez, *J. Comput. Chem.* **1989**, *11*, 205–216.
- [23] S. Pérez, F. R. Tavel, C. Vergelati, *Nouv. J. Chim.* **1985**, *9*, 561–564.
- [24] J. Dabrowski, T. Kozar, H. Grosskurth, N. E. Nifant'ev, *J. Am. Chem. Soc.* **1995**, *117*, 5534–5539.
- [25] C. Landersjö, R. Stenutz, G. Widmalm, *J. Am. Chem. Soc.* **1997**, *119*, 8695–8698.
- [26] J. F. Espinosa, M. Martin-Pastor, J. L. Asensio, H. Dietrich, M. Martin-Lomas, R. R. Schmidt, J. Jiménez-Barbero, *Tetrahedron Lett.* **1995**, *36*, 6329–6332.
- [27] a) M. Hricovini, R. N. Shah, J. P. Carver, *Biochemistry* **1992**, *3*, 10018–10023; b) T. J. Rutherford, J. Partridge, C. T. Weller, S. W. Homans, *Biochemistry* **1993**, *32*, 12715–12724; c) C. A. Bush, *Curr. Opin. Struct. Biol.* **1992**, *2*, 655–663; d) K. G. Rice, P. Wu, L. Brand, Y. C. Lee, *Curr. Opin. Struct. Biol.* **1993**, *3*, 669–674.
- [28] a) C. Mukhopadhyay, K. E. Miller, C. A. Bush, *Biopolymers* **1994**, *34*, 21–29; b) T. J. Rutherford, D. G. Spackman, P. J. Simpson, S. W. Homans, *Glycobiology* **1994**, *4*, 59–68; c) R. U. Lemieux, *Chem. Soc. Rev.* **1989**, *18*, 347–374; d) K. Bock, *Pure Appl. Chem.* **1983**, *55*, 605–622.
- [29] a) J. P. Carver, *Pure Appl. Chem.* **1993**, *65*, 763–770; b) A. Ejchart, J. Dabrowski, C. W. von der Lieth, *Magn. Reson. Chem.* **1992**, *30*, S105–S114; c) T. Peters, T. Weimar, *J. Biomol. NMR* **1994**, *4*, 97–116.
- [30] a) L. Poppe, H. van Halbeek, *J. Am. Chem. Soc.* **1992**, *114*, 1092–1094; b) M. Hricovini, G. Torri, *Carbohydr. Res.* **1995**, *268*, 159–175; c) B. J. Hardy, W. Egan, G. Widmalm, *Int. J. Biol. Macromol.* **1995**, *17*, 149–160; d) C. Meyer, S. Pérez, C. Hervé du Penhoat, V. Michon, *J. Am. Chem. Soc.* **1993**, *115*, 10300–10310; e) I. Braccini, V. Michon, C. Hervé du Penhoat, A. Imberty, S. Pérez, *Int. J. Biol. Macromol.* **1993**, *15*, 52–55; f) A. Poveda, J. L. Asensio, M. Martin-Pastor, J. Jiménez-Barbero, *Chem. Commun.* **1996**, 421–422; g) S. Bagley, H. Kovacs, J. Kowalewski, G. Widmalm, *Magn. Reson. Chem.* **1992**, *30*, 733–739; h) L. Maler, J. Lang, G. Widmalm, J. Kowalewski, *Magn. Reson. Chem.* **1995**, *33*, 541–548; i) J. F. Espinosa, J. L. Asensio, M. Bruix, J. Jiménez-Barbero, *An. Quim. Int. Ed.* **1996**, *96*, 320–324.
- [31] D. Neuhaus, M. P. Williamson, *The Nuclear Overhauser Effect in Structural and Conformational Analysis*, VCH, New York, **1989**.
- [32] G. Esposito, A. Pastore, *J. Magn. Reson.* **1988**, *76*, 331–336, and references therein.
- [33] a) H. Desvaux, P. Berthault, N. Bilirakis, M. Goldman, *J. Magn. Reson.* **1994**, *A108*, 219–229; b) G. Lippens, J. M. Wieruzeski, P. Talaga, J. P. Bohin, H. Desvaux, *J. Am. Chem. Soc.* **1996**, *118*, 7227–7228; c) D. G. Davis, *J. Am. Chem. Soc.* **1987**, *109*, 3471–3472; d) A. Poveda, J. L. Asensio, M. Martin-Pastor, J. Jiménez-Barbero, *J. Biomol. NMR* **1997**, *10*, 29–43.
- [34] a) K. Bock, J. Duus, *J. Carbohydr. Chem.* **1994**, *13*, 513–543; b) G. D. Rockwell, T. B. Grindley, *J. Am. Chem. Soc.* **1998**, *120*, 10953–10963.
- [35] J. H. Naismith, C. Emmerich, J. Habash, S. J. Harrop, J. R. Helliwell, W. N. Hunter, J. Raftery, A. J. (Gilboa) Kalb, J. Yariv, *Acta Crystallogr.* **1994**, *D50*, 847–848.
- [36] D. N. Moothoo, J. H. Naismith, *Glycobiology* **1998**, *8*, 173–181.

- [37] S. Pérez, C. Meyer, A. Imberty in: *Modelling of Biomolecular Structures and Mechanisms* (Eds.: A. Pullman, J. Jortner, B. Pullman), Kluwer Academic, Dordrecht, **1995**, pp. 425–454.
- [38] D. R. Bundle, R. Alibés, S. Nilar, A. Otter, M. Warwas, P. Zhang, *J. Am. Chem. Soc.* **1998**, *120*, 5317–5318.
- [39] J. Thomson, Y. F. Liu, J. M. Sturtevant, F. A. Quioco, *Biophys. Chem.* **1998**, *70*, 101–108.
- [40] Several other attempts have been reported to bias different structures towards the bioactive conformation; see: a) R. U. Lemieux, T. C. Wong, H. Thongersen, *Can. J. Chem.* **1982**, *60*, 81–86; b) K. Bock, J. O. Dues, O. Hindsgaul, I. Lindl, *Carbohydr. Res.* **1992**, *228*, 1–20; c) I. Lindh, O. Hindsgaul, *J. Am. Chem. Soc.* **1991**, *113*, 216–223; d) H. C. Kolb, B. Ernst, *Chem. Eur. J.* **1997**, *3*, 1571–1578; e) M. Wilstermann, J. Balogh, G. Magnusson, *J. Org. Chem.* **1997**, *62*, 3659–3665.
- [41] IUPAC-IUB Commission on Nomenclature: <http://www.chem.qm-w.ac.uk/iupac/>
- [42] a) T. Wiseman, S. Williston, J. F. Brandts, L.-N. Lin, *Analyt. Biochem.* **1989**, *179*, 131–137; b) A. Cooper, C. M. Johnson, in: *Microscopy, Optical Spectroscopy, and Macroscopic Techniques, Methods in Molecular Biology, Vol. 22* (Eds.: C. Jones, B. Mulloy, A. H. Thomas), Humana, Totowa, NJ, **1994**, pp. 137–150.
- [43] S. Pérez, M. M. Delage, *Carbohydr. Res.* **1991**, *212*, 523–529.
- [44] M. Clark, R. D. Cramer IV, N. van den Opdenbosch, *J. Comp. Chem.* **1989**, *10*, 982–1012.
- [45] F. P. Schwarz, K. D. Puri, R. G. Bhat, A. Surolia, *J. Biol. Chem.* **1995**, *268*, 7668–7677.
- [46] B. A. Williams, M. C. Chervenak, E. J. Toone, *J. Biol. Chem.* **1992**, *267*, 22907–22911.
- [47] D. K. Mandal, N. Kishore, C. F. Brewer, *Biochemistry* **1994**, *33*, 1149–1156.
- [48] M. C. Chervenak, E. J. Toone, *Biochemistry* **1995**, *34*, 5685–5695.

Received: October 5, 1998

Revised version: February 22, 1999 [F1370]